Assessing the impact of anthropogenic pollution on isoprene-derived secondary organic aerosol formation in $PM_{2.5}$ collected from the Birmingham, Alabama ground site during the 2013 Southern Oxidant and Aerosol Study

W. Rattanavaraha[1], K. Chu[1], S. H. Budisulistiorini[1,a], M. Riva[1], Y.-H. Lin[1,b], E. S. Edgerton[2], K. Baumann[2], S. L. Shaw[3], H. Guo[4], L. King[4], R. J. Weber[4], E. A. Stone[5], M. E. Neff[5], J. H. Offenberg[6], Z. Zhang[1], A. Gold[1], and J. D. Surratt[1,*]

[1] Department of Environmental Sciences and Engineering, Gillings School of Global Public Health, The University of North Carolina at Chapel Hill, Chapel Hill, NC, USA

[2] Atmospheric Research & Analysis, Inc., Cary, NC, USA

[3] Electric Power Research Institute, Palo Alto, CA, USA

[4] Earth and Atmospheric Science, Georgia Institute of Technology, Atlanta, GA, USA

[5] Department of Chemistry, University of Iowa, Iowa City, IA, USA

[6] Human Exposure and Atmospheric Sciences Division, United States Environmental Protection Agency, Research Triangle Park, NC, USA

[a] now at: Earth Observatory of Singapore, Nanyang Technological University, Singapore

[b] now at: Michigan Society of Fellows, Department of Chemistry, University of Michigan, Ann Arbor, MI, USA

* To whom correspondence should be addressed. Email: surratt@unc.edu

For Submission to: Atmospheric Chemistry & Physics Discussions

Abstract

In the southeastern U.S., substantial emissions of isoprene from deciduous trees undergo atmospheric oxidation to form secondary organic aerosol (SOA) that contributes to fine particulate matter ($PM_{2.5}$). Laboratory studies have revealed that anthropogenic pollutants, such as sulfur dioxide (SO_2), oxides of nitrogen (NO_x), and aerosol acidity, can enhance SOA formation from the hydroxyl radical (OH)-initiated oxidation of isoprene; however, the mechanisms by which specific pollutants enhance isoprene SOA in ambient $PM_{2.5}$ remain unclear. As one aspect of an investigation to examine how anthropogenic pollutants influence isoprene-derived SOA formation, high-volume $PM_{2.5}$ filter samples were collected at the Birmingham, Alabama (BHM) ground site during the 2013 Southern Oxidant and Aerosol Study (SOAS). Sample extracts were analyzed by gas chromatography/electron ionization-mass spectrometry (GC/EI-MS) with prior trimethylsilylation and ultra performance liquid chromatography coupled to electrospray ionization high-resolution quadrupole time-of-flight mass spectrometry (UPLC/ESI-HR-QTOFMS) to identify known isoprene SOA tracers. Tracers quantified using both surrogate and authentic standards were compared with collocated gas- and particle-phase data as well as meteorological data provided by the Southeastern Aerosol Research and Characterization (SEARCH) network to assess the impact of anthropogenic pollution on isoprene-derived SOA formation. Results of this study reveal that isoprene-derived SOA tracers contribute a substantial mass fraction of organic matter (OM) (~7 to ~20%). Isoprene-derived SOA tracers correlated with sulfate (SO_4^{2-}) ($r^2 = 0.34$, n = 117), but not with NO_x. Moderate correlation between methacrylic acid epoxide and hydroxymethyl-methyl-α-lactone (MAE/HMML)-derived SOA tracers with nitrate radical production ($P[NO_3]$) ($r^2 = 0.57$, n = 40) were observed during nighttime, suggesting a potential role of NO_3 radical in forming this SOA type. However, the nighttime correlation of

these tracers with nitrogen dioxide (NO_2) (r^2 = 0.26, n = 40) was weaker. Ozone (O_3) correlated strongly with MAE/HMML-derived tracers (r^2 = 0.72, n = 30) and moderately with 2-methyltetrols (r^2 = 0.34, n = 15) during daytime only, suggesting that a fraction of SOA formation could occur from isoprene ozonolysis in urban areas. No correlation was observed between aerosol pH and isoprene-derived SOA. Lack of correlation between aerosol acidity and isoprene-derived SOA is consistent with the observation that acidity is not a limiting factor for isoprene SOA formation at the BHM site as aerosols were acidic enough to promote multiphase chemistry of isoprene-derived epoxides throughout the duration of the study. All in all, these results confirm previous studies suggesting that anthropogenic pollutants enhance isoprene-derived SOA formation.

1. Introduction

Fine particulate matter, suspensions of liquid or solid aerosol in a gaseous medium that are less than or equal to 2.5 μm in diameter ($PM_{2.5}$), play a key role in physical and chemical atmospheric processes. They influence climate patterns both directly, through the absorption and scattering of solar and terrestrial radiation, and indirectly, through cloud formation (Kanakidou et al., 2005). In addition to climatic effects, $PM_{2.5}$ has been demonstrated to pose a human health risk through inhalation exposure (Pope and Dockery, 2006; Hallquist et al., 2009). Despite the strong association of $PM_{2.5}$ with climate change and environmental health, there remains a need to more fully resolve its composition, sources, and chemical formation processes in order to develop effective control strategies to address potential hazards in a cost-effective manner (Hallquist et al., 2009; Boucher et al., 2013; Nozière et al., 2015).

Atmospheric $PM_{2.5}$ are comprised in a large part (up to 90% by mass in some locations), of organic matter (OM) (Carlton et al., 2009; Hallquist et al., 2009). OM can be derived from many sources. Primary organic aerosol (POA) is emitted from both natural (e.g., fungal spores,

vegetation, vegetative detritus) and anthropogenic sources (fossil fuel and biomass burning) prior to atmospheric processing. As a result of large anthropogenic sources, POA is abundant largely in urban areas. Processes such as natural plant growth, biomass burning and combustion also yield volatile organic compounds (VOCs), which have high vapor pressures and can undergo atmospheric oxidation to form secondary organic aerosol (SOA) through gas-to-particle phase partitioning (condensation or nucleation) with subsequent particle-phase (multiphase) chemical reactions (Grieshop et al., 2009).

At around 600 Tg emitted per year into the atmosphere, isoprene (2-methyl-1,3-butadiene, C_5H_8) is the most abundant volatile non-methane hydrocarbon (Guenther et al., 2012). The abundance of isoprene is particularly high in the southeastern U.S. due to emissions from broadleaf deciduous tree species (Guenther et al., 2006). Research over the last decade has revealed that isoprene, via hydroxyl radical (OH)-initiated oxidation, is a major source of SOA (Claeys et al., 2004; Edney et al., 2005; Kroll et al., 2005 ; Kroll et al., 2006; Surratt et al., 2006; Lin et al., 2012; Lin et al., 2013a). In addition, it is known that SOA formation is enhanced by anthropogenic emissions, namely oxides of nitrogen (NO_x) and sulfur dioxide (SO_2), that are a source of acidic aerosol onto which photochemical oxidation products of isoprene are reactively taken up to yield a variety of SOA products (Edney et al., 2005; Kroll et al., 2006; Surratt et al., 2006; Surratt et al., 2007b; Surratt et al., 2010; Lin et al., 2013b;) .

Recent work has begun to elucidate some of the critical intermediates of isoprene oxidation that lead to SOA formation through acid-catalyzed heterogeneous chemistry (Kroll et al., 2005; Surratt et al., 2006). Under low-NO_x conditions, such as in a pristine environment, multiple isomers of isoprene epoxydiols (IEPOX) have been demonstrated to be critical to the formation of isoprene SOA. On advection of IEPOX to an urban environment and mixing with anthropogenic

emissions of acidic sulfate aerosol, SOA formation is enhanced (Surratt et al., 2006; Lin et al., 2012; Lin et al., 2013b). This pathway has been shown to yield 2-methyltetrols as major SOA constituents of ambient $PM_{2.5}$ (Claeys et al, 2004; Surratt et al., 2010; Lin et al., 2012). Further work has revealed a number of additional IEPOX-derived SOA tracers, including C_5-alkene triols (Wang et al., 2005; Lin et al., 2012), *cis*- and *trans*-3-methyltetrahydrofuran-3,4-diols (3-MeTHF-3,4-diols) (Lin et al., 2012; Zhang et al., 2012), IEPOX-derived organosulfates (OSs) (Lin et al., 2012), and IEPOX-derived oligomers (Lin et al., 2014). Some of the IEPOX-derived oligomers have been shown to contribute to aerosol components known as brown carbon that absorb light in the near ultraviolet (UV) and visible ranges (Lin et al., 2014). Under high-NO_x conditions, such as encountered in an urban environment, isoprene is oxidized to methacrolein and SOA formation occurs via the further oxidation of methacrolein (MACR) (Kroll et al., 2006; Surratt et al., 2006) to methacryloyl peroxynitrate (MPAN) (Chan et al., 2010; Surratt et al., 2010; Nguyen et al., 2015). It has recently been shown that when MPAN is oxidized by OH it yields at least two SOA precursors, methacrylic acid epoxide (MAE) and hydroxymethyl-methyl-α-lactone (HMML) (Surratt et al., 2006; Surratt et al., 2010; Lin et al., 2013a; Nguyen et al., 2015). Whether SOA precursors are formed under high- or low-NO_x conditions, aerosol acidity is a critical parameter that enhances the reaction kinetics through acid-catalyzed reactive uptake and multiphase chemistry of either IEPOX or MAE/HMML (Surratt et al., 2007b; Surratt et al., 2010; Lin et al., 2013b). In addition to MACR, other key oxidation products of isoprene, including glycolaldehyde, methylglyoxal, and hydroxyacetone, can undergo multiphase chemistry to yield their respective OS derivatives (Olsen et al., 2011; Schindelka et al. 2013; Shalamzari et al., 2013; Noziere et al., 2015). However, the contribution of isoprene on the glyoxal-, methylglyoxal-, and hydroxyacetone-derived OS mass concentrations in the atmosphere remains unclear since these

SOA tracers can also be formed from a wide variety of biogenic and anthropogenic precursors (Galloway et al., 2009, Liao et al., 2015).

Due to the large emissions of isoprene, an SOA yield of even 1% would contribute significantly to ambient SOA (Carlton et al., 2009; Henze et al., 2009). This conclusion is supported by measurements showing that up to a third of total fine OA mass can be attributed to IEPOX-derived SOA tracers in Atlanta, GA (JST) during summer months (Budisulistiorini et al., 2013; Budisulistiorini et al., 2015). A recent study in Yorkville, GA (YRK), similarly found that IEPOX-derived SOA tracers comprised 12-19% of the fine OA mass (Lin et al., 2013b). Another SOAS site at Centreville, Alabama (CTR) revealed IEPOX-SOA contributed 18% of total OA mass (Xu et al., 2015). The individual ground sites corroborate recent aircraft-based measurements made in the Studies of Emissions and Atmospheric Composition, Clouds, and Climate Coupling by Regional Surveys (SEAC4RS) aircraft campaign, which estimated an IEPOX-SOA contribution of 32% to OA mass in the southeastern U.S. (Hu et al., 2015).

It is clear from the field studies discussed above that particle-phase chemistry of isoprene-derived oxidation products plays a large role in atmospheric SOA formation. However, much remains unknown regarding the exact nature of its formation, limiting the ability of models to accurately account for isoprene SOA (Carlton et al., 2010b; Foley et al., 2010). Currently, traditional air quality models in the southeastern U.S. do not incorporate detailed particle-phase chemistry of isoprene oxidation products (IEPOX or MAE/HMML) and generally under-predict isoprene SOA formation (Carlton et al., 2010a). Recent work demonstrates that incorporating the specific chemistry of isoprene epoxide precursors into models increases the accuracy and amount of isoprene SOA predictions (Pye et al., 2013; Karambelas et al., 2014; McNeilll., 2015), suggesting that understanding the formation mechanisms of biogenic SOA, especially with regard

to the effects of anthropogenic emissions, such as NO_x and SO_2, will be key to more accurate models. More accurate models are needed in order to devise cost-effective control strategies for reducing $PM_{2.5}$ levels. Since isoprene is primarily biogenic in origin, and therefore not controllable, the key to understanding the public health and environmental implications of isoprene SOA lies in resolving the effects of anthropogenic pollutants.

This study presents results from the 2013 Southeastern Oxidant and Aerosol Study (SOAS), where several well-instrumented ground sites dispersed throughout the southeastern U.S. made intensive gas- and particle-phase measurements from June 1 – July 16, 2013. The primary purpose of this campaign was to examine, in greater detail, the formation mechanisms, composition, and properties of biogenic SOA, including the effects of anthropogenic emissions. This study pertains specifically to the results from the BHM ground site, where the city's ample urban emissions mix with biogenic emissions from the surrounding rural areas, creating an ideal location to investigate such interactions. The results presented here focus on analysis of $PM_{2.5}$ collected on filters during the campaign by GC/EI-MS and UPLC/ESI-HR-QTOFMS. The analysis of $PM_{2.5}$ was conducted in order to determine quantities of known isoprene SOA tracers and using collocated air quality and meteorological measurements to investigate how anthropogenic pollutants including NO_x, SO_2, aerosol acidity (pH), $PM_{2.5}$ sulfate (SO_4^{2-}), and O_3 affect isoprene SOA formation. These results, along with the results presented from similar studies during the 2013 SOAS campaign, seek to elucidate the chemical relationships between anthropogenic emissions and isoprene SOA formation in order to provide better parameterizations needed to improve the accuracy of air quality models in this region of the U.S.

2. Methods

2.1. Site description and collocated data

Filter samples were collected in the summer of 2013 as part of the SOAS field campaign at the BHM ground site (33.553N, 86.815W). In addition to the SOAS campaign, the site is also part of the Southeastern Aerosol Research and Characterization Study (SEARCH) (Figure S1 of the Supplement), an observation and monitoring program initiated in 1998. SEARCH and this site are described elsewhere in detail (Hansen et al., 2003; Edgerton et al., 2006). The BHM site is surrounded by significant transportation and industrial sources of PM. West of BHM are US-31 and I-65 highways. To the north, northeast and southwest of BHM several coking ovens and an iron pipe foundry are located (Hansen et al., 2003).

2.2. High-Volume filter sampling and analysis methods

2.2.1. High-Volume filter sampling

From June 1 – July 16, 2013, $PM_{2.5}$ samples were collected onto Tissuquartz^{TM} Filters (8 x 10 in, Pall Life Sciences) using high-volume $PM_{2.5}$ samplers (Tisch Environmental) operated at 1 m^3 min^{-1} at ambient temperature described in detail elsewhere (Budisulistiorini et al. 2015; Riva et al., 2016). All quartz filters were pre-baked prior to collection. The procedure consisted of baking filters at 550 °C for 18 hours followed by cooling to 25 °C over 12 hours.

The sampling schedule is given in Table 1. Either two or four samples were collected per day. The regular schedule consisted of two samples per day, one during the day, the second at night, each collected for 11 hours. On intensive sampling days, four samples were collected, with the single daytime sample being subdivided into three separate periods. The intensive sampling schedule was conducted on days when high levels of isoprene, SO_4^{2-} and NO_x were forecast by the National Center for Atmospheric Research (NCAR) using the Flexible Particle dispersion model (FLEXPART) (Stohl et al., 2005) and Model for Ozone and Related Chemical Tracers (MOZART)

(Emmons et al., 2010) simulations. Details of these simulations have been summarized in Budisulistiorini et al. (2015); however, these model data were only used qualitatively to determine the sampling schedule. The intensive collection frequency allowed enhanced time resolution for offline analysis to examine the effect of anthropogenic emissions on the evolution of isoprene SOA tracers throughout the day.

In total, 120 samples were collected throughout the field campaign with a field blank filter collected every 10 days to identify errors or contamination in sample collection and analysis. All filters were stored at -20 °C in the dark until extraction and analysis. In addition to filter sampling of $PM_{2.5}$, SEARCH provided a suite of additional instruments at the site that measured meteorological and chemical variables, including temperature, relative humidity (RH), trace gases (i.e., CO, O_3, SO_2, NO_x, and NH_3), and continuous PM monitoring. The exact variables measured with their respective instrumentation are summarized in Table S1 of the Supplement.

2.2.2. Isoprene-derived SOA analysis by GC/EI-MS

SOA collected in the field on quartz filters was extracted and isoprene tracers quantified by GC/EI-MS with prior trimethylsilylation. A 37-mm diameter circular punch from each filter was extracted in a pre-cleaned scintillation vial with 20 mL of high-purity methanol (LCMS CHROMASOLV-grade, Sigma-Aldrich) by sonication for 45 minutes. The extracts were filtered through polytetrafluorethylene (PTFE) syringe filters (Pall Life Science, Acrodisc®, 0.2-µm pore size) to remove insoluble particles and residual quartz fibers. The filtrate was then blown dry under a gentle stream of N_2 at room temperature. The dried residues were immediately trimethylsilylated by reaction with 100 μL of BSTFA + TMCS (99:1 *v/v*, Supelco) and 50 μL of pyridine (anhydrous, 99.8 %, Sigma-Aldrich) at 70 °C for 1 hour. Trimethylsilyl derivatives of carbonyl and hydroxyl functional groups were measurable by our GC/EI-MS method. Derivatized samples were analyzed

within 24 hours after trimethylsilylation using a Hewlett-Packard (HP) 5890 Series II Gas Chromatograph coupled to a HP 5971A Mass Selective Detector. The gas chromatograph was equipped with an *Econo-Cap®-EC®-5* Capillary Column (30 m x 0.25 mm i.d.; 0.25-μm film thickness) to separate trimethylsilyl derivatives before MS detection. 1 μL aliquots were injected onto the column. Operating conditions and procedures have been described elsewhere (Surratt et al., 2010).

Extraction efficiency was assessed and taken into account for the quantification of all SOA tracers. Efficiency was determined by analyzing 4 pre-baked filters spiked with 50 ppmv of 2-methyltetrols, 2-methylglyceric acid, levoglucosan, and *cis*- and *trans*-3-MeTHF-3,4-diols. Extraction efficiency was above 90% and used to correct the quantification of samples. Extracted ion chromatograms (EICs) of *m/z* 262, 219, 231, 335 were used to quantify the *cis*-/*trans*-3-MeTHF-3,4-diols, 2-methyltetrols and 2-methylglyceric acid, C_5-alkene triols, and IEPOX-dimers, respectively (Surratt et al., 2006).

2-Methyltetrols were quantified using an authentic reference standard that consisted of a mixture of racemic diasteroisomers. Similarly, 3-MeTHF-3,4-diol isomers were also quantified using authentic standards; however, 3-MeTHF-3,4-diol isomers were detected in few field samples. 2-Methylglyceric acid was also quantified using an authentic standard. Procedures for synthesis of the 2-methyltetrols, 3-MeTHF-3,4-diol isomers, and 2-methylglyceric acid have been described elsewhere (Zhang et al., 2012; Budisulistiorini et al., 2015). C_5-alkene triols and IEPOX-dimers were quantified using the average response factor of the 2-methyltetrols.

To investigate the effect of IEPOX-derived OS hydrolysis/decomposition during GC/EI-MS analysis, known concentrations (i.e., 1, 5, 10, and 25 pppv) of the authentic IEPOX-derived

OS standard (Budisulistiorini et al., 2015) were directly injected into the GC/MS following trimethylsilylation. Ratios of detected 2-methyltetrols to the IEPOX-derived OS were applied to estimate the total IEPOX-derived SOA tracers in order to avoid double counting when combining the GC/MS and UPLC/ESI-HR-QTOFMS SOA tracer results.

2.2.3. Isoprene-derived SOA analysis by UPLC/ ESI-HR-QTOFMS

A 37-mm diameter circular punch from each quartz filter was extracted following the same procedure as described in Section 2.2.2 for the GC/EI-MS analysis. However, after drying, the dried residues were instead reconstituted with 150 μl of a 50:50 (*v/v*) solvent mixture of methanol (LC-MS CHROMASOVL-grade, Sigma-Aldrich) and high-purity water (Milli-Q, 18.2 MΩ). The extracts were immediately analyzed by the UPLC/ESI-HR-QTOFMS (6520 Series, Agilent) operated in the negative ion mode. Detailed operating conditions have been described elsewhere (Riva et al., 2016). Mass spectra were acquired at a mass resolution 7000-8000.

Extraction efficiency was determined by analyzing 3 pre-baked filters spiked with propyl sulfate and octyl sulfate (electronic grade, City Chemical LLC). Extraction efficiencies were in the range 86 – 95%. EICs of *m/z* 215, 333 and 199 were used to quantify the IEPOX-derived OS, IEPOX-derived dimer OS and the MAE-derived OS, respectively (Surratt et al., 2007a). EICs were generated with a ± 5 ppm tolerance. Accurate masses for all measured organosulfates were within ± 5 ppm. For simplicity, only the nominal masses are reported in the text when describing these products. IEPOX-derived OS and IEPOX-derived dimer OS were quantified by the IEPOX-derived standard synthesized in-house (Budisulistiorini et al., 2015). The MAE-derived OS was quantified using an authentic MAE-derived OS standard synthesized in-house by a procedure to be described in a forthcoming publication (^{1}H NMR trace, Figure S2). Although the MAE-derived OS (Gómez-González et al., 2008), which is more formally called 3-sulfooxy-2-hydroxy-2-methyl

propanoic acid, has been chemically verified from the reactive uptake of MAE on wet acidic sulfate aerosol (Lin et al., 2013a), the term MAE/HMML-derived OS will be used hereafter to denote the two potential precursors (MAE and HMML) contributing to this OS derivative as recently discussed by Nguyen et al. (2015). It should be noted that Nguyen et al. (2015) provided indirect evidence for the possible existence of HMML. As a result, further work is needed to synthesize this compound to confirm its structure and likely role in SOA formation from isoprene oxidation.

EICs of of *m/z* 155, 169 and 139 were used to quantify the glyoxal-derived OS, methylglyoxal-derived OS, and the hydroxyacetone-derived OS, respectively (Surratt et al., 2007a). In addition, EICs of *m/z* 211, 260 and 305 were used to quantify other known isoprene-derived OSs (Surratt et al., 2007a). Glycolic acid sulfate synthesized in-house was used as a standard to quantify the glyoxal-derived OS (Galloway et al., 2009) and propyl sulfate, was used as a surrogate standard to quantify the remaining isoprene-derived OSs.

2.2.4. OC and WSOC analysis

A 1.5 cm^2 square punch from each quartz filter was analyzed for total organic carbon (OC) and elemental carbon (EC) by the thermal-optical method (Birch and Cary, 1996) on a Sunset Laboratory OC/EC instrument (Tigard, OR) at the National Exposure Research Laboratory (NERL) at the U.S. Environmental Protection Agency, Research Triangle Park, NC. The details of the instrument and analytical method have been described elsewhere (Birch and Cary, 1996). In addition to the internal calibration using methane gas, four different mass concentrations of sucrose solution were used to verify the accuracy of instrument during the analysis.

Water-soluble organic carbon (WSOC) was measured in aqueous extracts of quartz fiber filter samples using a total organic carbon (TOC) analyzer (Sievers 5310C, GE Water & Power) equipped with an inorganic carbon remover (Sievers 900). To maintain low background carbon

levels, all glassware used was washed with water, soaked in 10% nitric acid, and baked at 500 ˚C for 5 h and 30 min prior to use. Samples were extracted in batches that consisted of 12-21 $PM_{2.5}$ samples and field blanks, one laboratory blank, and one spiked solution. A 17.3 cm^2 filter portion was extracted with 15 mL of purified water (> 18 MΩ, Barnstead Easypure II, Thermo Scientific) by ultra-sonication (Branson 5510). Extracts were then passed through a 0.45 μm PTFE filter to remove insoluble particles. The TOC analyzer was calibrated using potassium hydrogen phthalate (KHP, Sigma Aldrich) and was verified daily with sucrose (Sigma Aldrich). Samples and standards were analyzed in triplicate; the reported values correspond to the average of the second and third trials. Spiked solutions yielded recoveries that averaged (± one standard deviation) 96 ± 5 % (n = 9). All ambient concentrations were field blank subtracted.

2.2.5. Estimation of aerosol pH by ISORROPIA

Aerosol pH was estimated using a thermodynamic model, ISORROPIA-II (Nenes et al., 1998). SO_4^{2-}, nitrate (NO_3^-), and ammonium (NH_4^+) ion concentrations measured in $PM_{2.5}$ collected from BHM, as well as relative humidity (RH), temperature and gas-phase ammonia (NH_3) were used as inputs into the model. These variables were obtained from the SEARCH network at BHM, which collected the data during the period covered by the SOAS campaign. The ISORROPIA-II model estimates particle hydronium ion concentration per unit volume of air (H^+, μg m^{-3}), aerosol liquid water content (LWC, μg m^{-3}), and aqueous aerosol mass concentration (μg m^{-3}). The model-estimated parameters were used in the following formula to calculate the aerosol pH:

$$\text{Aerosol pH} = -\log_{10} a_{H^+} = -\log_{10}\left(\frac{H^+_{air}}{LMASS} \times \rho_{aer} \times 1000\right)$$

where a_{H^+} is H^+ activity in the aqueous phase (mol L^{-1}), *LMASS* is total liquid-phase aerosol mass (μg m^{-3}) and ρ_{aer} is aerosol density. Details of the ISORROPIA-II model and its ability to predict pH, LWC, and gas-to-particle partitioning are not the focus of this study and are discussed elsewhere and (Fountoukis et al., 2009).

2.2.6. Estimation of nighttime NO_3

Nitrate radical (NO_3) production ($P[NO_3]$) was calculated using the following equation:

$$P[NO_3] = [NO_2][O_3]k$$

where $[NO_2]$ and $[O_3]$ correspond to the measured ambient NO_2 and O_3 concentrations (mol cm^{-3}), respectively, and *k* is the temperature-dependent rate constant (Herron and Huie, 1974; Graham and Johnston, 1978). Since no direct measure of NO_3 radical was made at this site during SOAS, $P[NO_3]$ was used as a proxy for NO_3 radicals present in the atmosphere to examine if there is any association of it with isoprene-derived SOA tracers.

3. Results and Discussion

3.1. Overview of the study

The campaign extended from June 1 through July 16, 2013. Temperature during this period ranged from a high of 32.6 °C to a low of 20.5 °C, with an average of 26.4 °C. RH varied from 37-96% throughout the campaign, with an average of 71.5%. Rainfall occurred intermittently over 2-3 day periods and averaged 0.1 inches per day. Wind analysis reveals that air masses approached largely from the south-southeast at an average wind speed of 2 m s^{-1}. Summaries of meteorological conditions as well as wind speed and direction during the course of the campaign are given in Table 2 and illustrated in Figures 1 and 2.

The average concentration of carbon monoxide (CO), a combustion byproduct, was 208.7 ppbv. The mean concentration of O_3 was significantly higher (t-test, *p-value* < 0.05) on intensive sampling days (37.0 ppbv) compared to regular sampling days (25.2 ppbv). Campaign average concentrations of NO_x, NH_3, and SO_2 were 7.8, 1.9, and 0.9 ppbv, respectively. On average, OC and WSOC levels were 7.2 (n = 120) and 4 μg m^{-3} (n = 100), respectively. The largest inorganic component of $PM_{2.5}$ was SO_4^{2-}, which averaged 2 μg m^{-3} with excursions between 0.4 and 4.9 μg m^{-3} during the campaign. NH_4^+ and NO_3^- were present at low levels, averaging 0.66 and 0.14 μg m^{-3}, respectively. Time series of gas and $PM_{2.5}$ components are shown in Figure 2. WSOC accounted for 35% of OC mass (Figure S3a), and was smaller than that recently reported in rural areas during SOAS (Budisulistiorini et al., 2015; Hu et al., 2015), but consistent with previous observations at the BHM site (Ding et al., 2008). WSOC/OC ratios are commonly lower in urban than rural areas, as a consequence of higher primary OC emissions; thus, PM at BHM probably contains increased OC.

Diurnal variation of meteorological parameters, trace gases, and $PM_{2.5}$ components are shown in Figure S4 of the Supplement. Temperature dropped during nighttime, and reached a maximum in the afternoon (Figure S4a). Conversely, RH was low during day and high at night. High NO_x levels were found in the early morning and decreased during the course of the day (Figure S4c), most likely due to forming NO_x sinks (e.g., $RONO_2$, $ROONO_2$, and HNO_3) as well as possibly due to increasing planetary boundary layer (PBL) heights. O_3 reached a maximum concentration between 12 - 3 pm due to photochemistry (Figure S4b). SO_2 was slightly higher in the morning (Figure S4c), but decreased during the day most likely as a result of PBL dynamics. NH_3 remained fairly constant throughout the day (Figure S4c). No significant diurnal variation was found in the concentration of inorganic $PM_{2.5}$ components, including SO_4^{2-}, NO_3^-, and NH_4^+

(Figure S4d). Unfortunately, a measurement of isoprene could not be made at BHM during the campaign. However, the diurnal trend of isoprene levels might be similar to the data at the CTR site (Xu et al., 2015), which is only 61 miles away from BHM. Xu et al. (2015) observed the highest levels of isoprene (~ 6 ppb) at CTR in the mid-afternoon (3 pm local time) and its diurnal trend was similar to isoprene-OA measured by the Aerodyne Aerosol Mass Spectrometer (AMS) during the SOAS campaign at the CTR site.

3.2 Characterization of Isoprene SOA

Table 3 summarizes the mean and maximum concentrations of known isoprene-derived SOA tracers detected by GC/EI-MS and UPLC/ESI-HR-QTOFMS. Levoglucosan was also analyzed as a tracer for biomass burning. Among the isoprene-derived SOA tracers, the highest mean concentration was for 2-methyltetrols (376 ng m^{-3}), followed by the sum of C_5-alkene triols (181 ng m^{-3}) and the IEPOX-derived OS (165 ng m^{-3}). The concentrations account for 3.8%, 1.8% and 1.6%, respectively, of total OM mass. Noteworthy is that maximum concentrations of 2-methylerythritol (a 2-methyltetrol isomer; 1049 ng m^{-3}), IEPOX-derived OS (865 ng m^{-3}) and (E)-2-methylbut-3-ene-1,2,4-triol (879 ng m^{-3}) were attained during the intensive sampling period 4-7 pm local time on June 15, 2013, following five consecutive days of dry weather (Figure 2a and 2d) when high levels of isoprene, SO_4^{2-}, and NO_x were forecast.

Our investigation for the potential of OS hydrolysis/decomposition during GC/EI-MS analysis demonstrated that only 1.7% of 2-methylthreitol and 2.4% of 2-methylerythritol could be derived from the IEPOX-derived OSs. In order to accurately estimate the mass concentrations of the IEPOX-derived SOA tracers, we took this effect into account. Together, the IEPOX-derived SOA tracers, which represent SOA formation from isoprene oxidation predominantly under the low-NO_x pathway, comprised 92.45% of the total detected isoprene-derived SOA tracer mass at

363 the BHM site. This contribution is slightly lower than observations reported at rural sites located
364 in Yorkville, GA (97.50%) and Look Rock, Tennessee (LRK) (97%) (Lin et al., 2013b;
365 Budisulistiorini et al., 2015).

366 The sum of MAE/HMML-OS and 2-MG, which represent SOA formation from isoprene
367 oxidation predominantly under the high-NO_x pathway, contributed 3.25% of the total isoprene-
368 derived SOA tracer mass, while the OS derivative of glycolic acid (GA sulfate) contributed 3.3%.
369 The contribution of GA sulfate was consistent with the level of GA sulfate measured by the
370 airborne NOAA Particle Analysis Laser Mass Spectrometer (PALMS) over the continental U.S.
371 during the Deep Convective Clouds and Chemistry Experiment and SEAC4RS (Liao et al., 2015).
372 However, the contribution of GA sulfate to the total OM at BHM (0.3%) is lower than aircraft-
373 based measurements made by Liao et al. (2015) near the ground in the eastern U.S. (0.9%). GA
374 sulfate can form from biogenic and anthropogenic emissions other than isoprene, including
375 glyoxal, which is thought to be a primary source of GA sulfate (Galloway et al., 2009). For this
376 reason, GA sulfate will not be further discussed in this study.

377 Isoprene SOA contribution to total OM was estimated by assuming the OM/OC ratio 1.6
378 based on recent studies (El-Zanan et al., 2009; Simon et al., 2011; Ruthenburg et al., 2014;
379 Blanchard et al., 2015). On average, isoprene-derived SOA tracers (sum of both IEPOX- and
380 MAE/HMML-derived SOA tracers) contributed ~7% (ranging up to ~ 20% at times) of the total
381 particulate OM mass. The average contribution is lower than measured at other sites in the S.E.
382 USA, including both rural LRK (Budisulistiorini et al., 2015; Hu et al., 2015) and urban Atlanta,
383 GA (Budisulistiorini et al., 2013). The contribution of SOA tracers to OM in the current study was
384 estimated on the basis of offline analysis of filters, while tracer estimates in the two earlier studies
385 were based on online ACSM/AMS measurements. The low isoprene SOA/OM ratio is consistent

386 with the low WSOC/OC reported in Section 3.1, suggesting a larger contribution of primary OA
387 or hydrophobic secondary OM originating from anthropogenic emissions to the total OM at BHM.
388 However, it should be noted that total IEPOX-derived SOA mass at BHM may actually be closer
389 to ~14% since recent measurements by the Aerodyne ACSM at LRK indicated that tracers could
390 only account for ~50% of the total IEPOX-derived SOA mass resolved by the ACSM
391 (Budisulistiorini et al., 2015). Unfortunately, an Aerodyne ACSM or AMS was not available at
392 the BHM site to support the confirmation that IEPOX-derived SOA mass at BHM might account
393 for 14% (on average) of the total OM mass.

394 Levoglucosan, a biomass-burning tracer, averaged 1% of total OM with spikes up to 8%,
395 the same level measured for 2-methylthreitol and (E)-2-methylbut-3-ene-1,2,4-triol (Table 3). The
396 ratio of average levoglucosan at BHM relative to CTR was 5.4, suggesting significantly more
397 biomass burning impacting the BHM site.

398 IEPOX- and MAE/HMML-derived SOA tracers accounted for 18% and 0.4% of the
399 WSOC mass, respectively (Figure S3b), lower than the respective contributions of 24% and 0.7%
400 measured at LRK (Budisulistiorini et al., 2015).

401 Figure 3 shows no difference for the average day and night concentration of isoprene-
402 derived SOA tracers, suggesting that the majority of isoprene SOA tracers are potentially long-
403 lived and formed upwind. A recent study by Lopez-Hilfiker et al. (2016) at the CTR site during
404 the 2013 SOAS demonstrated that isoprene-derived SOA was comprised of effectively nonvolatile
405 material, which could allow for this type of SOA to be long-lived in the atmosphere. Although 2-
406 MG and MAE-derived OS are known to form under high-NO_x conditions (Lin et al., 2013a), no
407 correlation between 2-MG and MAE-derived OS with NO_x (Table 4) is observed at the BHM. This

supports that isoprene SOA tracers likely formed at upwind locations and subsequently transported to the sampling site. Higher isoprene emissions during the daytime and cooler nighttime temperatures do not appear to cause any differences between daytime and nighttime isoprene-derived SOA tracer concentrations. Figures 4 and 5 show the variation of isoprene-derived SOA tracers during intensive sampling periods. The highest concentrations were usually observed in samples collected from 4 pm – 7 pm, local time; however, no statistical significance were observed between intensive periods. This observation illustrates the importance of the higher time-resolution of the tracer data during intensive sampling periods over course of the campaign (Table S2-S6). An additional consequence of the intensive sampling periods was resolution of a significant correlation between isoprene SOA tracers and O_3 to be discussed in more detail in Section 3.3.2.

3.3 Influence of anthropogenic emissions on isoprene-derived SOA

3.3.1 Effects of reactive nitrogen-containing species

During the campaign, no isoprene-derived SOA tracers, including MAE/HMML-derived OS and 2-MG, correlated with NO_x or NO_y ($r^2 = 0$, n = 120). This is inconsistent with the current understanding of SOA formation from isoprene oxidation pathways under high-NO_x conditions, which proceeds through uptake of MAE (Lin et al., 2013a), and, as recently suggested, HMML (Nguyen et al., 2015), to yield 2-MG and its OS derivative. Plume age, as a ratio of NO_x:NO_y, in this study was highly correlated with O_3 ($r^2 = 0.79$, n = 120) which is consistent with the relative diurnal variation of NO_x, NO_y, and O_3 as discussed in Section 3.1. This correlation might be also explained by the photolysis of NO_2, which is abundant due to traffic at the urban ground site, resulting in formation of tropospheric O_3. A negative correlation coefficient ($r^2 = 0.22$, n = 120) between plume age and 2-MG abundance was found as a consequence of relative diurnal variations. The peak of 2-MG was observed in the afternoon after NO_x has decreased. This

correlation leads to the hypothesis that the formation of 2-MG may be associated with ageing of air masses; however, further investigation is warranted. A previous study supported a major role for NO_3 in the nighttime chemistry of isoprene (Ng et al., 2008). Correlation of IEPOX- and MAE/HMML-derived SOA with nighttime NO_2, O_3, and $P[NO_3]$ were examined in this study (Figures 6 and 7). As shown in Figure 6f, a moderate correlation between MAE/HMML-derived SOA and nighttime $P[NO_3]$ ($r^2 = 0.57$, n = 40) was observed. The regression analysis revealed a significant correlation at the 95% confidence interval (*p-value* < 0.05) (Table S7). This finding suggests that some MAE/HMML-derived SOA may form locally from the reaction of isoprene with NO_3 radical at night. A field study reported a peak isoprene mixing ratio in early evening (Starn et al., 1998) as the PBL height decreases at night. As a result, lowering PBL heights could concentrate the remaining isoprene, NO_2, and O_3 that can continue to react during the course of the evening. 2-MG formation has been reported to be NO_2-dependent via the formation and further oxidation of MPAN (Surratt et al., 2006; Chan et al., 2010). Hence, decreasing PBL may be related to nighttime MAE/HMML-derived SOA formation through isoprene oxidation by both $P[NO_3]$ and NO_2.

Although $P[NO_3]$ depends on both NO_2 and O_3 levels, O_3 correlates moderately with MAE/HMML-derived SOA tracers during day ($r^2 = 0.48$, n = 75), but not at night ($r^2 = 0.08$, n = 45). The effect of O_3 on isoprene-derived SOA formation during daytime will be discussed further in Section 3.3.2. NO_2 levels correlate only weakly with MAE/HMML-derived SOA tracers ($r^2 = 0.26$, n = 45), indicating that NO_2 levels alone do not explain the moderate correlation of $P[NO_3]$ with these tracers. To our knowledge, correlation of $P[NO_3]$ with high-NO_x SOA tracers has not been observed in previous field studies, indicating that further work is needed to examine the potential role of nighttime NO_3 radicals in forming these SOA tracers.

As shown in Figure 7f, IEPOX-derived SOA was weakly correlated (r^2 = 0.26, n = 40) with nighttime P[NO_3]. The correlation appears to be driven by the data at the low end of the scale and could therefore be misleading. However, Schwantes et al. (2015) demonstrated that NO_3-initiated oxidation of isoprene yields isoprene nitrooxy hydroperoxides (INEs) through nighttime reaction of RO_2 + HO_2, which upon further oxidation yielded isoprene nitrooxy hydroxyepoxides (INHEs). The INHEs undergo reactive uptake onto acidic sulfate aerosol to yield SOA constituents similar to those of IEPOX-derived SOA. The present study raises the possibility that a fraction of IEPOX-derived SOA comes from NO_3-initiated oxidation of isoprene at night. The work of Ng et al. (2008), which only observed SOA as a consequence of the RO_2 + RO_2 and RO_2 + NO_3 reactions dominating the fate of the RO_2 radicals, does not explain the weak association between IEPOX-derived SOA tracers and P[NO3] we observe in this study. It is now thought that RO_2 + HO_2 should dominate the fate of RO_2 radicals in the atmosphere (Paulot et al., 2009; Schwantes et al., 2015).

3.3.2 Effect of O_3

During the daytime, O_3 was moderately correlated (r^2 = 0.48, n = 75) with total MAE/HMML-derived SOA (Figure 6b). This correlation was stronger (r^2 = 0.72, n = 30, *p-value* < 0.05, Table S7) when filters taken during regular daytime sampling periods are considered, suggesting that formation of MACR (a precursor to MAE and HMML) (Lin et al., 2013b; Nguyen et al., 2015) was enhanced by oxidation of isoprene by O_3 (Kamens et al., 1982). O_3 was not correlated (r^2 = 0.08, n = 45) with MAE/HMML-derived SOA at night (Figure 6e). The latter finding is consistent with the absence of photolysis to drive the production of O_3. However, residual O_3 may play an important role at night to form MAE/HMML-derived SOA via the P[NO_3] pathway discussed in Section 3.3.1.

O_3 was not correlated (r^2= 0.10, n = 75) with IEPOX-derived SOA during daytime (Figure 7b), but weakly correlated with 2-methylerythritol (r^2 = 0.25, n = 30) as shown in Table S2, especially during intensive 3 sampling periods (r^2 = 0.34, n = 15, Table S5). An important observation with regard to this result is that no correlation has been found between O_3 and 2-methyltetrols (r^2 < 0.01) in previous field studies (Lin et al., 2013b; Budisulistiorini et al., 2015). Isoprene ozonolysis yielded 2-methyltetrols in chamber studies in the presence of acidified sulfate aerosol (Riva et al., 2016), but C_5-alkene-triols were not formed by this pathway. The greatest abundance of isoprene-derived SOA tracers in daytime samples was generally observed in intensive 3 samples; however, there was no statistical significance observed between intensive samples. The moderate correlation (r^2 = 0.34, n = 15, *p-value* < 0.05) between O_3 and the 2-methyltetrols observed in intensive 3 samples occurred when O_3 reached maximum levels, suggesting that ozonolysis of isoprene plays a role in 2-methyltetrol formation. Lack of correlation between O_3 and C_5-alkene triols during intensive 3 sampling (r^2 = 0.10, n = 15) supports this contention. Previous studies (Nguyen et al., 2010; Inomata et al., 2014) proposed that SOA formation from isoprene ozonolysis occurs from stabilized Criegee intermediates (sCIs) that can further react in the gas phase to form higher molecular weight products that subsequently partition to the aerosol phase to make SOA. Recent work by Riva et al. (2016) systematically demonstrated that isoprene ozonolysis in the presence of wet acidic aerosol yields 2-methyltetrols and organosulfates unique to this process. Notably, no C_5-alkene triols were observed, which are known to form simultaneously with 2-methyltetrols if IEPOX multiphase chemistry is involved (Lin et al., 2012). Riva et al. (2016) tentatively proposed that hydroperoxides formed in the gas phase from isoprene ozonolysis potentially partition to wet acidic sulfate aerosols and hydrolyze to yield 2-methyltetrols as well as the unique set of organosulfates observed (Riva et al., 2016).

Additional work using authentic hydroperoxide standards is needed to validate this tentative hypothesis.

3.3.3 Effect of particle SO_4^{2-}

SO_4^{2-} was moderately correlated with IEPOX-derived SOA (r^2 = 0.36, n = 117) and MAE/HMML-derived SOA (r^2 = 0.33, n = 117) at the 95% confidence interval as shown in Table S7. The strength of the correlations was consistent with studies at other sites across the Southeastern U.S. (Budisulistiorini et al., 2013; Lin et al., 2013b; Budisulistiorini et al., 2015; Xu et al., 2015). Aerosol surface area provided by acidic SO_4^{2-} has been demonstrated to control the uptake of isoprene-derived epoxides (Lin et al., 2012; Gaston et al., 2014; Nguyen et al., 2014; Riedel et al., 2016).

Furthermore, SO_4^{2-} is proposed to enhance IEPOX-derived SOA formation by providing particle water (H_2O_{ptcl}) required for IEPOX uptake (Xu et al., 2015). Aerosol SO_4^{2-} also promotes acid-catalyzed ring-opening reactions of IEPOX by H^+, proton donors such as NH_4^+, and nucleophiles (e.g., H_2O, SO_4^{2-}, or NO_3^-) (Surratt et al., 2010; Nguyen et al., 2014). Since SO_4^{2-} tends to drive both particle water and acidity (Fountoukis and Nenes, 2007), the extent to which each influences isoprene SOA formation during field studies remains unclear. Multivariate linear regression analysis on SOAS data from the CTR site and the SCAPE dataset revealed a statistically significant positive linear relationship between SO_4^{2-} and the isoprene (IEPOX)-OA factor resolved by positive matrix factorization (PMF). On the basis of this analysis the abundance of SO_4^{2-} was concluded to control directly the isoprene SOA formation over broad areas of the Southeastern U.S. (Xu et al., 2015), consistent with previous reports (Lin et al., 2013; Budisulistiorini et al., 2013; Budisulistiorini et al., 2015). Another potential pathway for SO_4^{2-} levels to enhance isoprene SOA formation is through salting-in effects, which the solubility of

polar organic compounds would be increased in aqueous solution with increasing salt concentration (Xu et al., 2015). However, systematic investigations of this effect are lacking and further studies are warranted.

3.3.4 Effect of aerosol acidity

The aerosol at BHM was acidic throughout the SOAS campaign (pH range 1.60 – 1.94, average 1.76) in accord with a study by Guo et. al. (2014) that found aerosol pH ranging from 0 – 2 throughout the southeastern U.S. However, no correlation of pH with isoprene SOA formation was observed at BHM, also consistent with previous findings using the thermodynamic models to estimate aerosol acidity in many field sites across the southeastern U.S. region, including Yorkville, GA (YRK) (Lin et al., 2013b), Jefferson Street, GA (JST) (Budisulistiorini et al., 2013), and LRK (Budisulistiorini et al., 2015). However, it is important to point out that the lack of correlation between SOA tracers and acidity may stem from the small variations in aerosol acidity and the fact that aerosols are very acidic throughout the campaign. Gaston et al. (2014) and Riedel et al. (2015) recently demonstrated that an aerosol pH < 2 at atmospherically-relevant aerosol surface areas would allow reactive uptake of IEPOX onto acidic (wet) sulfate aerosol surfaces to be competitive with other loss processes (e.g., deposition and reaction of IEPOX with OH). In fact, it was estimated that under such conditions IEPOX would have a lifetime of ~ 5 hr. The constant presence of acidic aerosol has also been observed at other field sites in the southeastern U.S. (Budisulistiorini et al., 2013; Budisulistiorini et al., 2015; Xu et al., 2015), supporting a conclusion that acidity is not the limiting variable in forming isoprene SOA.

3.4 Comparison among different sampling sites during 2013 SOAS campaign

Table 5 summarizes the mean concentration and contribution of each isoprene SOA tracer at

BHM, CTR, and LRK. BHM is an industrial-residential area, LRK and CTR are rural areas, although LRK is influenced by a diurnal upslope/downslope cycle of air from an urban locality (Knoxville) (Tanner et al., 2005). IEPOX-derived SOA (isoprene SOA produced under low-NO_x conditions) was predominant at all three sites during the SOAS campaign, while MAE/HMML-derived SOA (isoprene SOA produced under high-NO_x conditions) constituted a minor contribution. The average ratio of 2-methyltetrols to C_5-alkene triols at BHM was 2.2, nearly double that of CTR (1.3) and LRK (1.1). Although 2-methyltetrols and C_5-alkene triols are considered to form readily from the acid-catalyzed reactive uptake and multiphase chemistry of IEPOX (Edney et al., 2005; Surratt et al., 2006), Riva et al. (2016) recently demonstrated that only 2-methyltetrols can be formed via isoprene ozonolysis in the presence of acidic sulfate aerosol. The detailed mechanism explaining isoprene ozonolysis is still unclear, but acid-catalyzed heterogeneous reaction with organic peroxides or H_2O_2 was considered to be possible routes for 2-methyltetrol formation. The higher levels of the 2-methyltetrols observed at the urban BHM site indicates a likely competition between the IEPOX uptake and ozonolysis pathways. Together, these findings suggest that urban O_3 may play an important role in forming the 2-methyltetrols observed at BHM. There were notable trends found among the three sites: (1) average C_5-alkene triol concentrations were higher at CTR (214.1 ng m^{-3}) than at BHM (169.7 ng m^{-3}) and LRK (144.4 ng m^{-3}); (2) average isomeric 3-MeTHF-diol concentrations were lower at CTR (0.2 ng m^{-3}) than the BHM (15.4 ng m^{-3}) or LRK (4.4 ng m^{-3}) sites. Except for the 2-methyltetrols, reasons for the differences observed for the other tracers between sites remains unclear and warrant future investigations.

4. Conclusions

This study examined isoprene SOA tracers in $PM_{2.5}$ samples collected at the BHM ground site during the 2013 SOAS campaign and revealed the complexity and potential multitude of chemical pathways leading to isoprene SOA formation. Isoprene SOA contributed up to ~20% (~7% on average) of total OM mass. IEPOX-derived SOA tracers were responsible for 92.45% of the total quantified isoprene SOA tracer mass, with 2-methyltetrols being the major component (47%). Differences in the relative contributions of IEPOX- and MAE/HMML-derived SOA tracers at BHM and the rural CTR and LRK sites (Budisulistiorini et al., 2015) during the 2013 SOAS campaign, support suggestions that anthropogenic emissions affect isoprene SOA formation. The correlation between 2-methyltetrols and O_3 at BHM is in accord with work by Riva et al. (2016), demonstrating a potential role of O_3 in generating isoprene-derived SOA in addition to the currently accepted IEPOX multiphase pathway.

At BHM, the statistical correlation of particulate SO_4^{2-} with IEPOX- ($r^2 = 0.36$, n = 117, $p < 0.05$) and MAE-derived SOA tracers ($r^2 = 0.33$, n = 117, $p < 0.05$) suggests that SO_4^{2-} plays a role in isoprene SOA formation. Although none of isoprene-derived SOA tracers correlated with gas-phase NO_x and NO_y, MAE/HMML-derived SOA tracers correlated with nighttime $P[NO_3]$ ($r^2 = 0.57$, n = 40), indicating that NO_3 may affect local MAE/HMML-derived SOA formation. Nighttime $P[NO_3]$ was weakly correlated ($r^2 = 0.26$, n = 40) with IEPOX-derived SOA tracers, lending some support to recent work by Schwantes et al. (2015) showing that isoprene + NO_3 yields INHEs that can by undergo reactive uptake to yield IEPOX tracers and contribute to IEPOX-derived SOA tracer loadings. The correlation of daytime O_3 with MAE/HMML-derived SOA and with 2-methyltetrols offers a new insight into influences on isoprene SOA formation. Notably, O_3 has not been reported to correlate with isoprene-derived SOA tracers in previous field studies (Lin

et al., 2013b; Budisulistiorini et al., 2015). In this study, the strong correlation (r^2 = 0.72, n = 30) at the 95% confidence interval of O_3 with MAE/HMML-derived SOA tracers during the regular daytime sampling schedule indicates that O_3 likely oxidizes some isoprene to MACR as precursor of 2-MG at BHM. The weak correlation (r^2 = 0.16, n = 75) between O_3 and 2-methyltetrols early in the day as well as the better correlation (r^2 = 0.34, n = 15) later in the day (intensive 3, 4-7 PM local time) are consistent with recent laboratory studies demonstrating that 2-methyltetrols can be formed via isoprene ozonolysis in the presence of acidified sulfate aerosol (Riva et al., 2016).

Although urban O_3 and nighttime $P[NO_3]$ may have a role in local formation of MAE/HMML- and IEPOX-derived SOA tracers at BHM, this does not appear to explain the majority of the SOA tracers, since no significant day-night variation of the entire group of tracers was observed during the campaign. The majority of IEPOX-derived SOA was likely formed when isoprene SOA precursors (IEPOX) were generated upwind and transported to the BHM site. Wind directions during the campaign are consistent with long-range transport of isoprene SOA precursors from southwest of the site, which is covered by forested areas. The absence of a correlation of aerosol acidity with MAE/HMML- and IEPOX-derived SOA tracers indicates that acidity is not the limiting variable that controls formation of these compounds. Because the aerosols are acidic (campaign average aerosol pH of 1.8), the lack of correlation between SOA tracers and acidity may stem from the nearly invariant aerosol acidity throughout the campaign. Hence, despite laboratory studies demonstrating that aerosol acidity can enhance isoprene SOA formation (Surratt et al., 2007; Surratt et al., 2010; Lin et al., 2012), the effect may not be significant in the southeastern U.S. during the summer months due to the constant acidity of aerosols. Future work should examine how well current models can predict the isoprene SOA levels observed during this study, especially in the presence of fresh urban emissions.

Furthermore, explicit models are now available to predict the isoprene SOA tracers measured here (McNeill et al., 2012; Pye et al., 2013), which will allow the modeling community to test the current parameterizations that are used to capture the enhancing effect of anthropogenic pollutants on isoprene-derived SOA formation. In addition, the significant correlations of isoprene-derived SOA tracers with $P[NO_3]$ observed during this study indicate a need to better understand nighttime chemistry of isoprene. Lastly, although O_3 appears to have an enhancing effect on isoprene-derived SOA tracers, the intermediates are unknown. Hydroperoxides suggested by Riva et al. (2016) may be key, but chamber experiments with authentic precursors are needed to test this hypothesis.

Acknowledgements

This work was funded by the U.S. Environmental Protection Agency (EPA) through grant number 835404. The contents of this publication are solely the responsibility of the authors and do not necessarily represent the official views of the U.S. EPA. Further, the U.S. EPA does not endorse the purchase of any commercial products or services mentioned in the publication. The authors would also like to thank the Electric Power Research Institute (EPRI) for their support. This study was supported in part by the National Oceanic and Atmospheric Administration (NOAA) Climate Program Office's AC4 program, award number NA13OAR4310064. The authors thank the Camille and Henry Dreyfus Postdoctoral Fellowship Program in Environmental Chemistry for their financial support. The authors thank Louisa Emmons and Christoph Knote for their assistance with chemical forecasts made available during the SOAS campaign. We would like to thank Annmarie Carlton, Joost deGouw, Jose Jimenez, and Allen Goldstein for helping to organize the SOAS campaign and coordinating communication between ground sites. UPLC/ESI-HR-Q-TOFMS analyses were conducted in the UNC-CH Biomarker Mass Facility located within the Department of Environmental Sciences and Engineering, which is a part of the UNC-CH Center for Environmental Health and Susceptibility supported by National Institute for Environmental Health Sciences (NIEHS), grant number 5P20-ES10126. WSOC measurements at the University of Iowa were supported through EPA STAR grant 8354101. The authors thank Theran Riedel for useful discussions. We also thank SCG Chemicals Co., Ltd., Siam Cement Group, Thailand, for the full support for W. Rattanavaraha attending UNC, Chapel Hill.

643 **References**

644 Birch, M. E., and Cary, R. A.: Elemental carbon-based method for occupational monitoring of
645 particulate diesel exhaust: methodology and exposure issues, Analyst, 121, 1183-1190,
646 1996.

647 Blanchard, C. L., Hidy, G. M., Shaw, S., Baumann, K., and Edgerton, E. S.: Effects of emission
648 reductions on organic aerosol in the southeastern United States, Atmos. Chem. Phys.
649 Discuss., 15, 17051-17092, doi:10.5194/acpd-15-17051-2015, 2015.

650 Boucher, O., Randall, D., Artaxo, P., Bretherton, C., Feingold, G., Forster, P., Kerminen, V.-M.,
651 Kondo, Y., Liao, H., and Lohmann, U.: Clouds and aerosols, in: Climate change 2013:
652 the physical science basis. Contribution of Working Group I to the Fifth Assessment
653 Report of the Intergovernmental Panel on Climate Change, Cambridge University Press,
654 571-657, 2013.

655 Budisulistiorini, S. H., Canagaratna, M. R., Croteau, P. L., Marth, W. J., Baumann, K., Edgerton,
656 E. S., Shaw, S. L., Knipping, E. M., Worsnop, D. R., and Jayne, J. T.: Real-time
657 continuous characterization of secondary organic aerosol derived from isoprene
658 epoxydiols in downtown Atlanta, Georgia, using the Aerodyne Aerosol Chemical
659 Speciation Monitor, Environ. Sci. Technol., 47, 5686-5694, 2013.

660 Budisulistiorini, S., Li, X., Bairai, S., Renfro, J., Liu, Y., Liu, Y., McKinney, K., Martin, S.,
661 McNeill, V., and Pye, H.: Examining the effects of anthropogenic emissions on isoprene-
662 derived secondary organic aerosol formation during the 2013 Southern Oxidant and
663 Aerosol Study (SOAS) at the Look Rock, Tennessee, ground site, Atmos. Chem. Phys.
664 Discuss., 15, 7365-7417, 2015.

665 Carlton, A., Wiedinmyer, C., and Kroll, J.: A review of Secondary Organic Aerosol (SOA)
666 formation from isoprene, Atmos. Chem. Phys, 9, 4987-5005, 2009.

667 Carlton, A. G., Bhave, P. V., Napelenok, S. L., Edney, E. O., Sarwar, G., Pinder, R. W., Pouliot,
668 G. A., and Houyoux, M.: Model representation of secondary organic aerosol in CMAQv4.
669 7, Environ. Sci. Technol., 44, 8553-8560, 2010a.

670 Carlton, A. G., Pinder, R. W., Bhave, P. V., and Pouliot, G. A.: To what extent can biogenic SOA
671 be controlled?, Environ. Sci. Technol., 44, 3376-3380, 2010b.

672 Chan, A., Chan, M., Surratt, J., Chhabra, P., Loza, C., Crounse, J., Yee, L., Flagan, R., Wennberg,
673 P., and Seinfeld, J.: Role of aldehyde chemistry and NOx concentrations in secondary
674 organic aerosol formation, Atmos. Chem. Phys, 10, 7169-7188, 2010.
675 Claeys, M., Graham, B., Vas, G., Wang, W., Vermeylen, R., Pashynska, V., Cafmeyer, J., Guyon,
676 P., Andreae, M. O., and Artaxo, P.: Formation of secondary organic aerosols through
677 photooxidation of isoprene, Science, 303, 1173-1176, 2004.
678 Ding, X., Zheng, M., Yu, L., Zhang, X., Weber, R. J., Yan, B., Russell, A. G., Edgerton, E. S., and
679 Wang, X.: Spatial and seasonal trends in biogenic secondary organic aerosol tracers and
680 water-soluble organic carbon in the southeastern United States, Environ. Sci. Technol.,
681 42, 5171-5176, 2008.
682 Edgerton, E. S., Hartsell, B. E., Saylor, R. D., Jansen, J. J., Hansen, D. A., and Hidy, G. M.: The
683 Southeastern Aerosol Research and Characterization Study, part 3: Continuous
684 measurements of fine particulate matter mass and composition, J.Air Waste
685 Manag.Assoc., 56, 1325-1341, 2006.
686 Edney, E. O., Kleindienst, T. E., Jaoui, M., Lewandowski, M., Offenberg, J. H., Wang, W., and
687 Claeys, M.: Formation of 2-methyl tetrols and 2-methylglyceric acid in secondary organic
688 aerosol from laboratory irradiated isoprene/NO_X/SO_2/air mixtures and their detection in
689 ambient PM2.5 samples collected in the eastern United States, Atmos. Environ., 39, 5281-
690 5289, http://dx.doi.org/10.1016/j.atmosenv.2005.05.031, 2005.
691 El-Zanan, H. S., Zielinska, B., Mazzoleni, L. R., and Hansen, D. A.: Analytical determination of
692 the aerosol organic mass-to-organic carbon ratio, J.Air Waste Manag.Assoc., 59, 58-69,
693 2009.
694 Emmons, L. K., Walters, S., Hess, P. G., Lamarque, J. F., Pfister, G. G., Fillmore, D., Granier, C.,
695 Guenther, A., Kinnison, D., Laepple, T., Orlando, J., Tie, X., Tyndall, G., Wiedinmyer,
696 C., Baughcum, S. L., and Kloster, S.: Description and evaluation of the Model for Ozone
697 and Related chemical Tracers, version 4 (MOZART-4), Geosci. Model Dev., 3, 43-67,
698 10.5194/gmd-3-43-2010, 2010.
699 Foley, K., Roselle, S., Appel, K., Bhave, P., Pleim, J., Otte, T., Mathur, R., Sarwar, G., Young, J.,
700 and Gilliam, R.: Incremental testing of the Community Multiscale Air Quality (CMAQ)
701 modeling system version 4.7, Geosci. Model Dev, 3, 205-226, 2010.

Fountoukis, C., and Nenes, A.: ISORROPIA II: a computationally efficient thermodynamic equilibrium model for K+–Ca 2+–Mg 2+–NH 4+–Na+–SO 4 2−–NO 3−–Cl−–H 2 O aerosols, Atmos. Chem. Phys, 7, 4639-4659, 2007.

Fountoukis, C., Nenes, A., Sullivan, A., Weber, R., Reken, T. V., Fischer, M., Matias, E., Moya, M., Farmer, D., and Cohen, R.: Thermodynamic characterization of Mexico City aerosol during MILAGRO 2006, Atmos. Chem. Phys, 9, 2141-2156, 2009.

Galloway, M. M., Chhabra, P. S., Chan, A. W. H., Surratt, J. D., Flagan, R. C., Seinfeld, J. H., and Keutsch, F. N.: Glyoxal uptake on ammonium sulphate seed aerosol: reaction products and reversibility of uptake under dark and irradiated conditions, Atmos. Chem. Phys., 9, 3331-3345, 10.5194/acp-9-3331-2009, 2009.

Gómez-González, Y., Surratt, J. D., Cuyckens, F., Szmigielski, R., Vermeylen, R., Jaoui, M., Lewandowski, M., Offenberg, J. H., Kleindienst, T. E., Edney, E. O., Blockhuys, F., Van Alsenoy, C., Maenhaut, W., and Claeys, M.: Characterization of organosulfates from the photooxidation of isoprene and unsaturated fatty acids in ambient aerosol using liquid chromatography/(-) electrosprayionization massspectrometry, J.MassSpectrom.,43,371–382, 2008.

Graham, R. A., and Johnston, H. S.: The photochemistry of the nitrate radical and the kinetics of the nitrogen pentoxide-ozone system, J.Phys. Chem., 82, 254-268, 1978.

Guenther, A. B., Jiang, X., Heald, C. L., Sakulyanontvittaya, T., Duhl, T., Emmons, L. K., and Wang, X.: The Model of Emissions of Gases and Aerosols from Nature version 2.1 (MEGAN2.1): an extended and updated framework for modeling biogenic emissions, Geosci Model Dev, 5, 1471-1492, 10.5194/gmd-5-1471-2012, 2012.

Grieshop, A., P., Logue, J., M., Donahue., J., M., and Robinson, A., L.: Laboratory investigation of photochemical oxidation of organic aerosol from wood fires 1 : measurement and simulation of organic aerosol evolution, Atmos. Chem. Phys., 9, 1263-1277, 2009.

Hallquist, M., Wenger, J. C., Baltensperger, U., Rudich, Y., Simpson, D., Claeys, M., Dommen, J., Donahue, N. M., George, C., Goldstein, A. H., Hamilton, J. F., Herrmann, H., Hoffmann, T., Iinuma, Y., Jang, M., Jenkin, M. E., Jimenez, J. L., Kiendler-Scharr, A., Maenhaut, W., McFiggans, G., Mentel, T. F., Monod, A., Prévôt, A. S. H., Seinfeld, J. H., Surratt, J. D., Szmigielski, R., and Wildt, J.: The formation, properties and impact of

secondary organic aerosol: current and emerging issues, Atmos. Chem. Phys., 9, 5155-5236, 10.5194/acp-9-5155-2009, 2009.

Hansen, D. A., Edgerton, E. S., Hartsell, B. E., Jansen, J. J., Kandasamy, N., Hidy, G. M., and Blanchard, C. L.: The Southeastern aerosol research and characterization study: part 1—overview, J.Air Waste Manag.Assoc., 53, 1460-1471, 2003.

Henze, D. K., Seinfeld, J. H., and Shindell, D. T.: Inverse modeling and mapping US air quality influences of inorganic PM 2.5 precursor emissions using the adjoint of GEOS-Chem, Atmos. Chem. Phys., 9, 5877-5903, 2009.

Herron, J. T., and Huie, R. E.: Rate constants for the reactions of ozone with ethene and propene, from 235.0 to 362.0. deg. K, J.Phys. Chem, 78, 2085-2088, 1974.

Hu, W., Campuzano-Jost, P., Palm, B., Day, D., Ortega, A., Hayes, P., Krechmer, J., Chen, Q., Kuwata, M., and Liu, Y.: Characterization of a real-time tracer for Isoprene Epoxydiols-derived Secondary Organic Aerosol (IEPOX-SOA) from aerosol mass spectrome-ter measurements, Atmos. Chem. Phys. Discuss., 15, 11223-11276, 2015.

Inomata, Satoshi, Kei Sato, Jun Hirokawa, Yosuke Sakamoto, Hiroshi Tanimoto, Motonori Okumura, Susumu Tohno, and Takashi Imamura. Analysis of secondary organic aerosols from ozonolysis of isoprene by proton transfer reaction mass spectrometry. Atmos Environ., 97, 397-405, 2014.

Kamens, R., Gery, M., Jeffries, H., Jackson, M., and Cole, E.: Ozone-isoprene reactions: product formation and aerosol potential, Int. J. Chem. Kinet., 14, 955-975, 1982.

Kanakidou, M., Seinfeld, J. H., Pandis, S. N., Barnes, I., Dentener, F. J., Facchini, M. C., Van Dingenen, R., Ervens, B., Nenes, A., Nielsen, C. J., Swietlicki, E., Putaud, J. P., Balkanski, Y., Fuzzi, S., Horth, J., Moortgat, G. K., Winterhalter, R., Myhre, C. E. L., Tsigaridis, K., Vignati, E., Stephanou, E. G., and Wilson, J.: Organic aerosol and global climate modelling: a review, Atmos. Chem. Phys., 5, 1053-1123, 10.5194/acp-5-1053-2005, 2005.

Karambelas, A., Pye, H. O., Budisulistiorini, S. H., Surratt, J. D., and Pinder, R. W.: Contribution of isoprene epoxydiol to urban organic aerosol: evidence from modeling and measurements, Environ. Sci. Technol. Lett., 1, 278-283, 2014.

761 Kroll, J. H., Ng, N. L., Murphy, S. M., Flagan, R. C., and Seinfeld, J. H.: Secondary organic aerosol
762 formation from isoprene photooxidation under high-NOx conditions, Geophys. Res. Lett.,
763 32, 2005.
764 Kroll, J. H., Ng, N. L., Murphy, S. M., Flagan, R. C., and Seinfeld, J. H.: Secondary Organic
765 Aerosol Formation from Isoprene Photooxidation, Environ. Sci. Technol., 40, 1869-1877,
766 10.1021/es0524301, 2006.
767 Liao, J., Froyd, K. D., Murphy, D. M., Keutsch, F. N., Yu, G., Wennberg, P. O., St Clair, J. M.,
768 Crounse, J. D., Wisthaler, A., and Mikoviny, T.: Airborne measurements of
769 organosulfates over the continental US, J.Geophys Res A., 120, 2990-3005, 2015.
770 Lin, Y.-H., Zhang, Z., Docherty, K. S., Zhang, H., Budisulistiorini, S. H., Rubitschun, C. L., Shaw,
771 S. L., Knipping, E. M., Edgerton, E. S., and Kleindienst, T. E.: Isoprene epoxydiols as
772 precursors to secondary organic aerosol formation: acid-catalyzed reactive uptake studies
773 with authentic compounds, Environ. Sci. Technol., 46, 250-258, 2012.
774 Lin, Y.-H., Zhang, H., Pye, H. O., Zhang, Z., Marth, W. J., Park, S., Arashiro, M., Cui, T.,
775 Budisulistiorini, S. H., and Sexton, K. G.: Epoxide as a precursor to secondary organic
776 aerosol formation from isoprene photooxidation in the presence of nitrogen oxides, Proc.
777 Natl. Acad. Sci., 110, 6718-6723, 2013a.
778 Lin, Y. H., Knipping, E. M., Edgerton, E. S., Shaw, S. L., and Surratt, J. D.: Investigating the
779 influences of SO_2 and NH_3 levels on isoprene-derived secondary organic aerosol
780 formation using conditional sampling approaches, Atmos. Chem. Phys., 13, 8457-8470,
781 10.5194/acp-13-8457-2013, 2013b.
782 Lin, Y.-H., Budisulistiorini, S. H., Chu, K., Siejack, R. A., Zhang, H., Riva, M., Zhang, Z., Gold,
783 A., Kautzman, K. E., and Surratt, J. D.: Light-absorbing oligomer formation in secondary
784 organic aerosol from reactive uptake of isoprene epoxydiols, Environ. Sci. Technol., 48,
785 12012-12021, 2014.
786 Lopez-Hilfiker, F. D., Claudia Mohr, Emma L. D'Ambro, Anna Lutz, Theran P. Riedel, Cassandra
787 J. Gaston, Siddharth Iyer et al.: Molecular Composition and Volatility of Organic Aerosol
788 in the Southeastern US: Implications for IEPOX Derived SOA. Environ. Sci.
789 Technol., 50, no. 5, 2200-2209, 2016.
790 McNeill, V. F., Woo, J. L., Kim, D. D., Schwier, A. N., Wannell, N. J., Sumner, A. J., & Barakat,
791 J. M.: Aqueous-phase secondary organic aerosol and organosulfate formation in

792 atmospheric aerosols: a modeling study, Environ. Sci. Technol., 46(15), 8075-8081,
793 2012.
794 McNeill, V. F. Aqueous organic chemistry in the atmosphere: Sources and chemical processing of
795 organic aerosols. Environ. Sci. Technol., 49(3), 1237-1244, 2015.
796 Nenes, A., Pandis, S. N., and Pilinis, C.: ISORROPIA: A new thermodynamic equilibrium model
797 for multiphase multicomponent inorganic aerosols, Aqua. Geo., 4, 123-152, 1998.
798 Ng, N., Kwan, A., Surratt, J., Chan, A., Chhabra, P., Sorooshian, A., Pye, H., Crounse, J.,
799 Wennberg, P., and Flagan, R.: Secondary organic aerosol (SOA) formation from reaction
800 of isoprene with nitrate radicals (NO_3), Atmos. Chem. Phys., 8, 4117-4140, 2008.
801 Nguyen, Tran B., Adam P. Bateman, David L. Bones, Sergey A. Nizkorodov, Julia Laskin, and
802 Alexander Laskin. High-resolution mass spectrometry analysis of secondary organic
803 aerosol generated by ozonolysis of isoprene. Atmos. Environ. 44, no. 8, 1032-1042, 2010.
804 Nguyen, T., Coggon, M., Bates, K., Zhang, X., Schwantes, R., Schilling, K., Loza, C., Flagan, R.,
805 Wennberg, P., and Seinfeld, J.: Organic aerosol formation from the reactive uptake of
806 isoprene epoxydiols (IEPOX) onto non-acidified inorganic seeds, Atmos. Chem. Phys,
807 14, 3497-3510, 2014.
808 Nguyen, T. B., Bates, K. H., Crounse, J. D., Schwantes, R. H., Zhang, X., Kjaergaard, H. G.,
809 Surratt, J. D., Lin, P., Laskin, A., and Seinfeld, J. H.: Mechanism of the hydroxyl radical
810 oxidation of methacryloyl peroxynitrate (MPAN) and its pathway toward secondary
811 organic aerosol formation in the atmosphere, PCCP, 17, 17914-17926, 2015.
812 Nozière, B., Kalberer, M., Claeys, M., Allan, J., D'Anna, B., Decesari, S., Finessi, E., Glasius,
813 M., Grgić, I., and Hamilton, J. F.: The Molecular Identification of Organic Compounds
814 in the Atmosphere: State of the Art and Challenges, Chem. Rev., 10.1021/cr5003485,
815 2015.
816 Olson, C. N., Galloway, M. M., Yu, G., Hedman, C. J., Lockett, M. R., Yoon, T., ... & Keutsch,
817 F. N.: Hydroxycarboxylic acid-derived organosulfates: synthesis, stability, and
818 quantification in ambient aerosol. Environ. Sci. Technol., 45(15), 6468-6474, 2011.
819 Paulot, F., Crounse, J. D., Kjaergaard, H. G., Kürten, A., Clair, J. M. S., Seinfeld, J. H., &
820 Wennberg, P. O.: Unexpected epoxide formation in the gas-phase photooxidation of
821 isoprene. Science, 325(5941), 730-733, 2009.

822 Pope, C. A., and Dockery, D. W.: Health Effects of Fine Particulate Air Pollution: Lines that
823 Connect, J.Air Waste Manag. Assoc., 56, 709-742, 10.1080/10473289.2006.10464485,
824 2006.
825 Pye, H. O., Pinder, R. W., Piletic, I. R., Xie, Y., Capps, S. L., Lin, Y.-H., Surratt, J. D., Zhang, Z.,
826 Gold, A., and Luecken, D. J.: Epoxide pathways improve model predictions of isoprene
827 markers and reveal key role of acidity in aerosol formation, Environ. Sci. Technol., 47,
828 11056-11064, 2013.
829 Riedel, T. P., Lin, Y.-H., Budisulistiorini, S. H., Gaston, C. J., Thornton, J. A., Zhang, Z., Vizuete,
830 W., Gold, A., and Surratt, J. D.: Heterogeneous reactions of isoprene-derived epoxides:
831 reaction probabilities and molar secondary organic aerosol yield estimates, Environ. Sci.
832 Technol. Lett, 2, 38-42, 2015.
833 Riva, M., Budisulistiorini, S. H., Zhang, Z., Gold, A., and Surratt, J. D.: Chemical characterization
834 of secondary organic aerosol constituents from isoprene ozonolysis in the presence of
835 acidic aerosol, Atmos. Environ., 130, 5-13, 2016.
836 Ruthenburg, T. C., Perlin, P. C., Liu, V., McDade, C. E., and Dillner, A. M.: Determination of
837 organic matter and organic matter to organic carbon ratios by infrared spectroscopy with
838 application to selected sites in the IMPROVE network, Atmos. Environ., 86, 47-57, 2014.
839 Schindelka, J., Iinuma, Y., Hoffmann, D., & Herrmann, H.: Sulfate radical-initiated formation of
840 isoprene-derived organosulfates in atmospheric aerosols. Fara. discuss., 165, 237-259,
841 2013.
842 Schwantes, R. H., Teng, A. P., Nguyen, T. B., Coggon, M. M., Crounse, J. D., St. Clair, J. M.,
843 Zhang, X., Schilling, K. A., Seinfeld, J. H., and Wennberg, P. O.: Isoprene NO_3 Oxidation
844 Products from the RO_2+ HO_2 Pathway, J.Phys. Chem. A, 2015.
845 Shalamzari, M., Ryabtsova, O., Kahnt, A., Vermeylen, R., Hérent, M.-F., Quetin-Leclercq, J., Van
846 der Veken, P., Maenhaut, W. and Claeys, M.: Mass spectrometric characterization of
847 organosulfates related to secondary organic aerosol from isoprene. Rapid Commun. Mass
848 Spectrom., 27: 784–794. doi:10.1002/rcm.6511, 2013.
849 Simon, H., Bhave, P. V., Swall, J. L., Frank, N. H., and Malm, W. C.: Determining the spatial and
850 seasonal variability in OM/OC ratios across the US using multiple regression, Atmos.
851 Chem. Phys., 11, 2933-2949, 10.5194/acp-11-2933-2011, 2011.

852 Starn, T., Shepson, P., Bertman, S., Riemer, D., Zika, R., and Olszyna, K.: Nighttime isoprene
853 chemistry at an urban-impacted forest site, J.Geo. Res. A. (1984–2012), 103, 22437-
854 22447, 1998.
855 Stohl, A., Forster, C., Frank, A., Seibert, P., and Wotawa, G.: Technical note: The Lagrangian
856 particle dispersion model FLEXPART version 6.2, Atmos. Chem. Phys., 5, 2461-2474,
857 10.5194/acp-5-2461-2005, 2005.
858 Surratt, J. D., Murphy, S. M., Kroll, J. H., Ng, N. L., Hildebrandt, L., Sorooshian, A., Szmigielski,
859 R., Vermeylen, R., Maenhaut, W., and Claeys, M.: Chemical composition of secondary
860 organic aerosol formed from the photooxidation of isoprene, J.Phys. Chem. A, 110, 9665-
861 9690, 2006.
862 Surratt, J. D., Kroll, J. H., Kleindienst, T. E., Edney, E. O., Claeys, M., Sorooshian, A., Ng, N. L.,
863 Offenberg, J. H., Lewandowski, M., and Jaoui, M.: Evidence for organosulfates in
864 secondary organic aerosol, Environ. Sci. Technol., 41, 517-527, 2007a.
865 Surratt, J. D., Lewandowski, M., Offenberg, J. H., Jaoui, M., Kleindienst, T. E., Edney, E. O., and
866 Seinfeld, J. H.: Effect of acidity on secondary organic aerosol formation from isoprene,
867 Environ. Sci. Technol., 41, 5363-5369, 2007b.
868 Surratt, J. D., Chan, A. W., Eddingsaas, N. C., Chan, M., Loza, C. L., Kwan, A. J., Hersey, S. P.,
869 Flagan, R. C., Wennberg, P. O., and Seinfeld, J. H.: Reactive intermediates revealed in
870 secondary organic aerosol formation from isoprene, Proc. Natl. Acad. Sci., 107, 6640-
871 6645, 2010.
872 Tanner, R. L., Bairai, S. T., Olszyna, K. J., Valente, M. L., and Valente, R. J.: Diurnal patterns in
873 PM 2.5 mass and composition at a background, complex terrain site, Atmos. Environ.,
874 39, 3865-3875, 2005.
875 Wang, W., Kourtchev, I., Graham, B., Cafmeyer, J., Maenhaut, W., and Claeys, M.:
876 Characterization of oxygenated derivatives of isoprene related to 2-methyltetrols in
877 Amazonian aerosols using trimethylsilylation and gas chromatography/ion trap mass
878 spectrometry, Rapid Commun. Mass Spectrom., 19, 1343-1351, 2005.
879 Xu, L., Guo, H., Boyd, C. M., Klein, M., Bougiatioti, A., Cerully, K. M., Hite, J. R., Isaacman-
880 VanWertz, G., Kreisberg, N. M., and Knote, C.: Effects of anthropogenic emissions on
881 aerosol formation from isoprene and monoterpenes in the southeastern United States,
882 Proc. Natl. Acad. Sci., 112, 37-42, 2015.

883 Zhang, Z., Lin, Y.-H., Zhang, H., Surratt, J., Ball, L., and Gold, A.: Technical Note: Synthesis of
884 isoprene atmospheric oxidation products: isomeric epoxydiols and the rearrangement
885 products *cis*-and *trans*-3-methyl-3,4-dihydroxytetrahydrofuran, Atmos. Chem. Phys., 12,
886 8529-8535, 2012.

887 **Table 1.** Sampling schedule during SOAS at the BHM ground site.

No. of samples/ day	Sampling schedule	Dates
2 (regular)	Day: 8 am – 7 pm Night: 8 pm – 7 am next day	June 1 – June 9 June 13, June 17 – June 28, July 2- July 9, July 15
4 (intensive)	Intensive 1: 8 am – 12 pm, Intensive 2: 1 pm – 3 pm, Intensive 3: 4 pm – 7 pm, Intensive 4: 8 pm – 7 am next day	June 10 – June 12, June 14 – June 16, June 29 – June 30, July 1, July 9 – July 14

888

889 **Table 2.** Summary of collocated measurements of meteorological variables, gaseous species, and
890 $PM_{2.5}$ constituents.

891

Category	Condition	Average	SD	Minimum	Maximum
Meteorology	Rainfall (in)	0.1	0.2	0.0	1.4
	Temp (°C)	26.4	3.0	20.5	32.7
	RH (%)	71.5	15.0	36.9	96.1
	BP (mbar)	994.2	3.9	984.2	1002.4
	SR (W m^{-2})	303.7	274.5	7.0	885.0
Trace gas (ppbv)	O_3	31.1	14.8	8.3	62.2
	CO	208.7	72.0	99.6	422.9
	SO_2	0.9	0.8	0.1	3.7
	NO	1.3	1.2	0.1	7.0
	NO_2	6.6	5.1	1.0	22.7
	NO_x	7.8	6.0	1.3	29.7
	NO_y	9.1	5.8	2.2	30.4
	HNO_3	0.3	0.2	0.1	1.0
	NH_3	1.9	0.8	0.7	4.0
$PM_{2.5}$ (μg m^{-3})	OC	7.2	3.2	1.4	14.9
	EC	0.6	0.5	0.1	2.7
	WSOC	4.0	1.8	0.5	7.5
	SO_4^{2-}	2.0	0.9	0.4	4.9
	NO_3^-	0.1	0.1	0.0	0.8
	NH_4^+	0.7	0.3	0.2	1.2
	Aerosol pH	1.8	0.1	1.6	1.9

Table 3. Summary of isoprene-derived SOA tracers measured by GC/EI-MS and UPLC/ESI-HR-QTOFMS

SOA tracers	*m/z*	Frequency of detection (%)[a]	Max concentration (ng/m^3)	Mean concentration (ng/m^3)	Isoprene SOA Mass fraction (%)[b]	% of total OM[c]
Measured by GC/EI-MS						
2-methylerythritol[d]	219	99.2	1048.9	269.0	33.8	2.7
2-methylthreitol[d]	219	100.0	388.9	107.3	13.5	1.1
(E)-2-methylbut-3-ene-1,2,4-triol[e]	231	96.7	878.9	112.7	14.2	1.1
(Z)-2-methylbut-3-ene-1,2,4-triol[e]	231	95.8	287.8	38.9	4.9	0.4
2-methylbut-3-ene-1,2,3-triol[e]	231	94.2	503.3	28.9	3.6	0.3
2-methylglyceric acid[d]	219	93.3	35.0	10.8	1.4	0.1
cis-3-MeTHF-3,4-diol[d]	262	22.5	98.9	6.9	0.9	0.1
trans-3-MeTHF-3,4-diol[d]	262	10.0	137.6	8.6	1.1	0.1
IEPOX-derived dimer[e]	333	10.0	2.2	0.0	0.0	0.0
Levoglucosan[d]	204	100.0	922.6	98.7	-	1.0
Measured by UPLC/ESI-HR-QTOFMS						
IEPOX-derived OSs						
$C_5H_{11}O_7S^-$[d]	215	100.0	864.9	164.5	20.7	1.6
$C_{10}H_{21}O_{10}S^-$[f]	333	1.7	0.3	0.0	0.0	0.0
MAE-derived OS[d]						
$C_4H_7O_7S^-$	199	100.0	35.7	7.2	1.9	0.1
GA sulfate[d]						
$C_2H_3O_6S^-$	155	100.0	75.2	26.2	3.3	0.3
Methylglyoxal-derived OS[g]						
$C_3H_5O_6S^-$	169	97.5	10.5	2.7	0.3	0.0
Isoprene-derived OSs[g]						
$C_5H_7O_7S^-$	211	97.5	5.2	1.4	0.2	0.0
$C_5H_{10}NO_9S^-$	260	90.0	3.9	0.3	0.0	0.0
$C_5H_9N_2O_{11}S^-$	305	5.0	3.3	2.9	0.4	0.0
Hydroxyacetone-derived OS[g]						
$C_2H_3O_5S^-$	139	30.8	2.6	0.2	0.0	0.0

[a] Total filters = 120

[b] Mass fraction is the contribution of each species among total known isoprene-derived SOA mass detected by GC/EI MS and UPLC/ESI-HR-QTOFMS

[c] OM/OC = 1.6

[d] OA tracers quantified by authentic standards

[e] SOA tracers quantified by 2-methyltetrols as a surrogate standard

[f] SOA tracer quantified by IEPOX-derived OS (*m/z* 215) as a surrogate standard

[g] SOA tracers quantified by propyl sulfate as a surrogate standard

899 **Table 4.** Overall correlation (r^2) of isoprene-derived SOA tracers and collocated measurements at
900 BHM during 2013 SOAS campaign.

SOA tracers	**CO**	**O_3**	**NO_x**	**NO_y**	**SO_2**	**NH_3**	**SO_4**	**NO_3**	**NH_4**	**OC**	**WSOC**	**pH**
MAE/HMML-derived SOA tracers*	**0.07**	**0.26**	**0.00**	**0.01**	**0.06**	**0.11**	**0.33**	**0.01**	**0.18**	**0.47**	**0.20**	**0.00**
2-methylglyceric acid	0.01	0.26	0.01	0.00	0.01	0.07	0.10	0.00	0.06	0.19	0.02	0.00
MAE-derived OS	0.10	0.14	0.00	0.02	0.07	0.09	0.38	0.01	0.18	0.32	0.23	0.01
IEPOX-derived SOA tracers**	**0.04**	**0.05**	**0.00**	**0.01**	**0.05**	**0.01**	**0.36**	**0.00**	**0.21**	**0.24**	**0.12**	**0.00**
2-methylerythritol	0.00	0.16	0.03	0.02	0.01	0.00	0.30	0.02	0.18	0.18	0.19	0.00
2-methylthreitol	0.00	0.13	0.02	0.03	0.02	0.00	0.20	0.01	0.16	0.17	0.15	0.00
(E)-2-methylbut-3-ene-1,2,4-triol	0.07	0.00	0.02	0.01	0.07	0.00	0.15	0.00	0.19	0.11	0.04	0.00
(Z)-2-methylbut-3-ene-1,2,4-triol	0.04	0.00	0.00	0.00	0.06	0.00	0.28	0.00	0.20	0.04	0.00	0.00
2-methylbut-3-ene-1,2,3-triol	0.02	0.00	0.03	0.00	0.00	0.02	0.32	0.01	0.03	0.17	0.04	0.00
IEPOX-derived OS	0.02	0.14	0.03	0.00	0.00	0.00	0.27	0.00	0.16	0.29	0.29	0.00
IEPOX dimer	0.00	0.00	0.00	0.00	0.00	0.00	0.00	0.00	0.00	0.00	0.00	0.00
Other isoprene SOA tracers												
GA sulfate												
$C_2H_3O_6S^-$	0.30	0.23	0.01	0.00	0.08	0.09	0.27	0.00	0.19	0.38	0.18	0.00
Methylglyoxal-derived OS												
$C_3H_5O_6S^-$	0.14	0.04	0.02	0.03	0.03	0.07	0.31	0.02	0.25	0.21	0.24	0.00
Isoprene-derived OSs												
$C_5H_7O_7S^-$	0.01	0.23	0.03	0.01	0.00	0.02	0.21	0.00	0.16	0.31	013	0.00
$C_5H_{10}NO_9S^-$	0.17	0.00	0.12	0.14	0.10	0.14	0.31	0.16	0.23	0.20	0.07	0.00
$C_5H_9N_2O_{11}S^-$ ***	0.32	0.71	0.66	0.58	0.42	0.02	0.68	0.50	0.42	0.00	0.50	0.00
Hydroxyacetone-derived OS												
$C_2H_3O_5S^-$	0.02	0.10	0.08	0.07	0.05	0.00	0.00	0.03	0.00	0.01	0.01	0.00
Other tracer												
Levoglucosan	0.00	0.09	0.02	0.01	0.02	0.00	0.00	0.02	0.00	0.08	0.04	0.01

901 * Summed tracers for MAE/HMML-derived SOA
902 ** Summed tracers for IEPOX-derived SOA
903 ***Found only in 6 of 120 filters
904 The correlations in this table are positive.

905

Table 5. Summary of isoprene-derived SOA tracers from the three SOAS ground sites: BHM, CTR, and LRK.

SOA tracers	Urban		Rural			
	BHM		CTR		LRK	
	Mean (ng m^{-3})	Average fraction of detected tracers (%)	Mean (ng m^{-3})	Average fraction of detected tracers (%)	Mean (ng m^{-3})	Average fraction of detected tracers (%)
MAE/HMML derived SOA						
MAE/HMML-derived OS	7.2	1.1	10.2	1.3	8.2	1.8
2-methylglyceric acid	10.4	1.7	5.1	0.7	7.5	1.6
IEPOX derived SOA						
IEPOX-derived OS	164.5	24.3	207.1	26.8	139.2	30.3
IEPOX-derived dimer OS	0.04	0.00	0.7	0.1	1.1	0.2
2-methylerythritol	266.7	37.9	204.8	26.5	120.7	26.3
2-methylthreitol	107.3	15.8	73.7	9.5	42.4	9.2
(E)-2-methylbut-3-ene-1,2,4-triol	109.0	12.3	137.3	17.8	98.8	21.5
(Z)-2-methylbut-3-ene-1,2,4-triol	37.3	4.1	50.7	6.6	29.1	6.1
2-methylbut-3-ene-1,2,3-triol	23.4	2.5	26.1	3.4	16.5	3.6
trans-3-MeTHF-3,4-diol	8.6	1.0	0.0	0.0	2.7	0.6
cis-3-MeTHF-3,4-diol	6.8	1.0	0.2	0.0	1.7	0.4

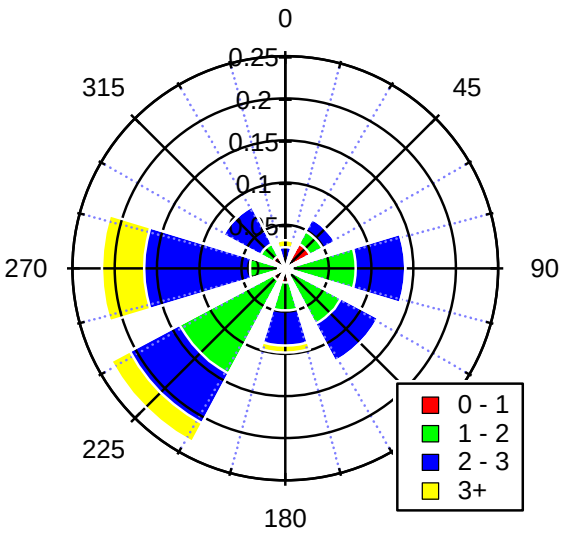

Figure 1. Wind rose illustrating wind direction during the campaign at the BHM site. Bars indicate direction of incoming wind, with 0 degrees set to geographic north. Length of bar size indicates frequency with color segments indicating the wind speed in m s^{-1}.

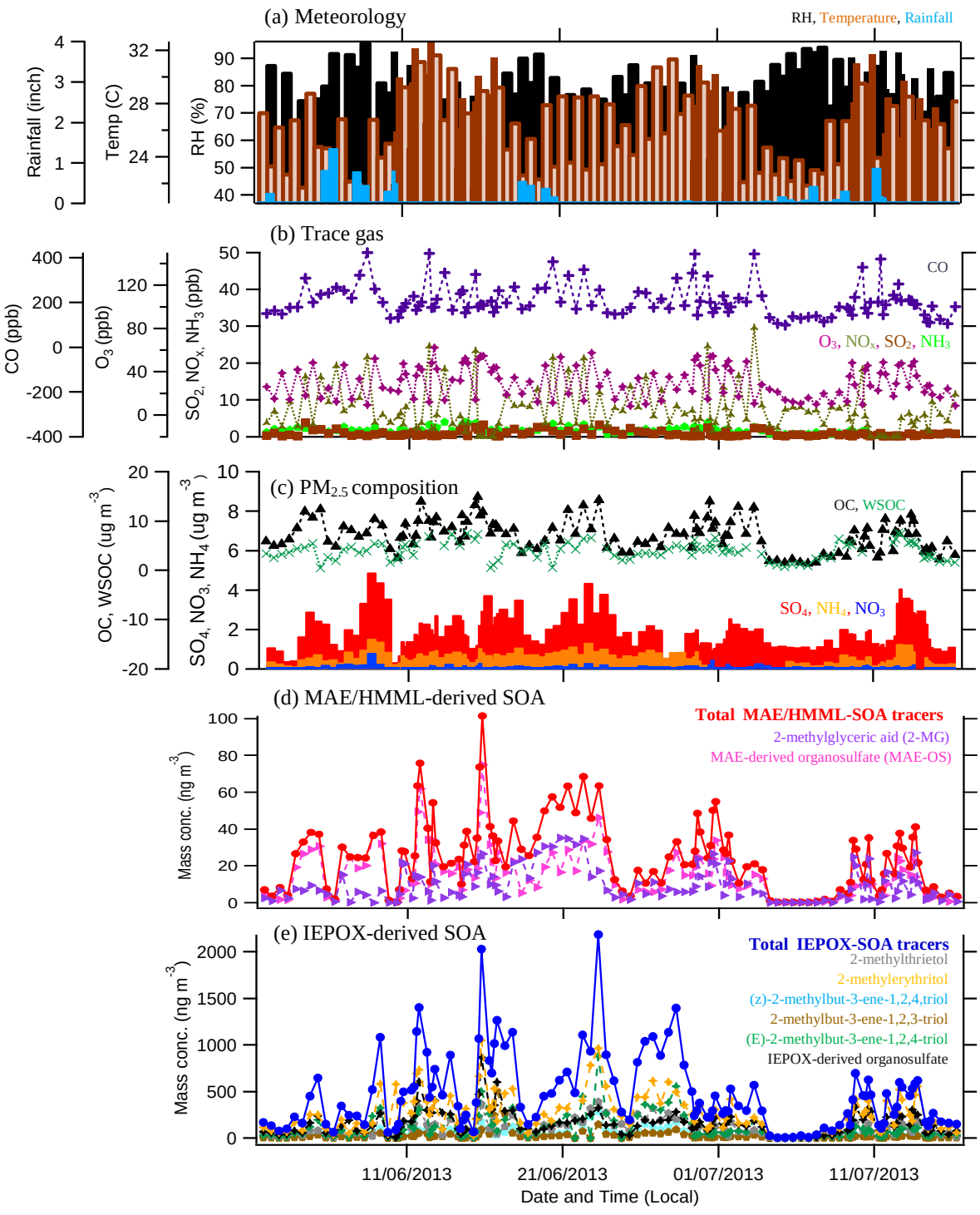

Figure 2. Time series of (a) meteorological data, (b) trace gases, (c) $PM_{2.5}$ constituents, (d) MAE/HMML-derived SOA tracers and (e) IEPOX-derived SOA tracers during the 2013 SOAS campaign at the BHM site.

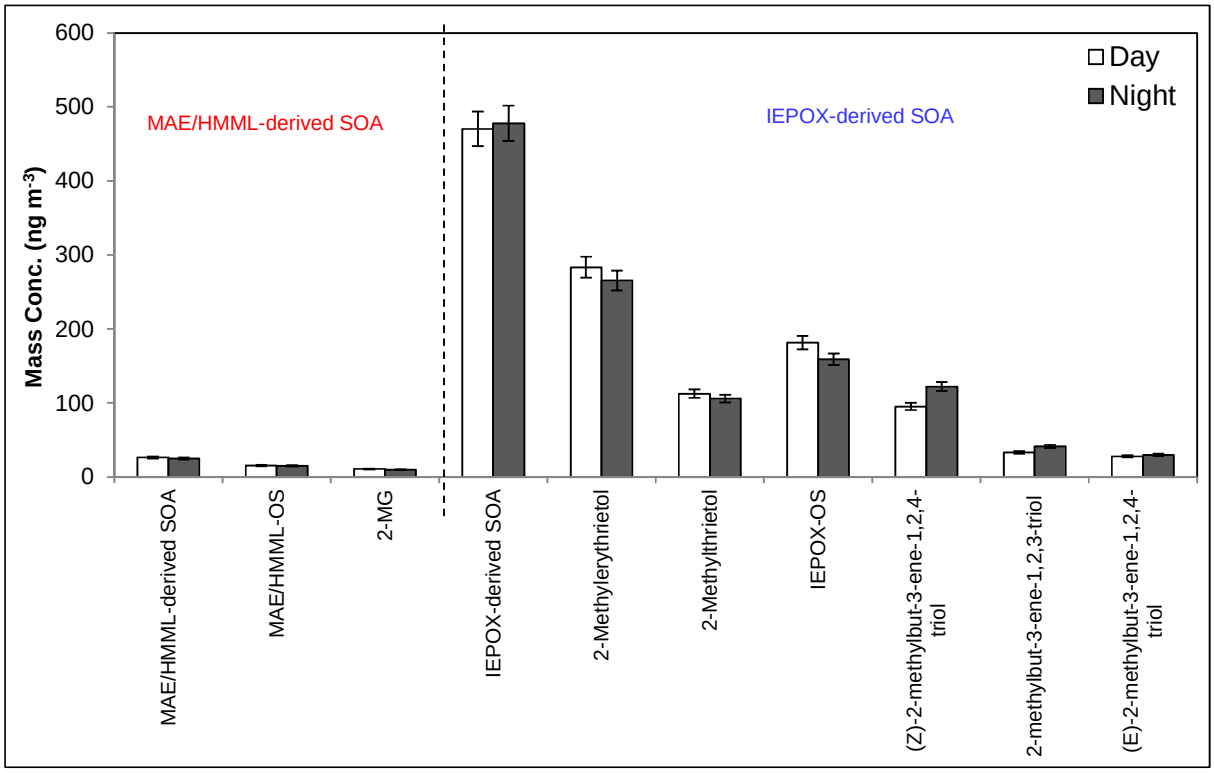

Figure 3. The bar chart shows average daytime and nighttime concentrations of isoprene-derived SOA tracers with 95% confident interval. No significant variation between daytime and nighttime was observed.

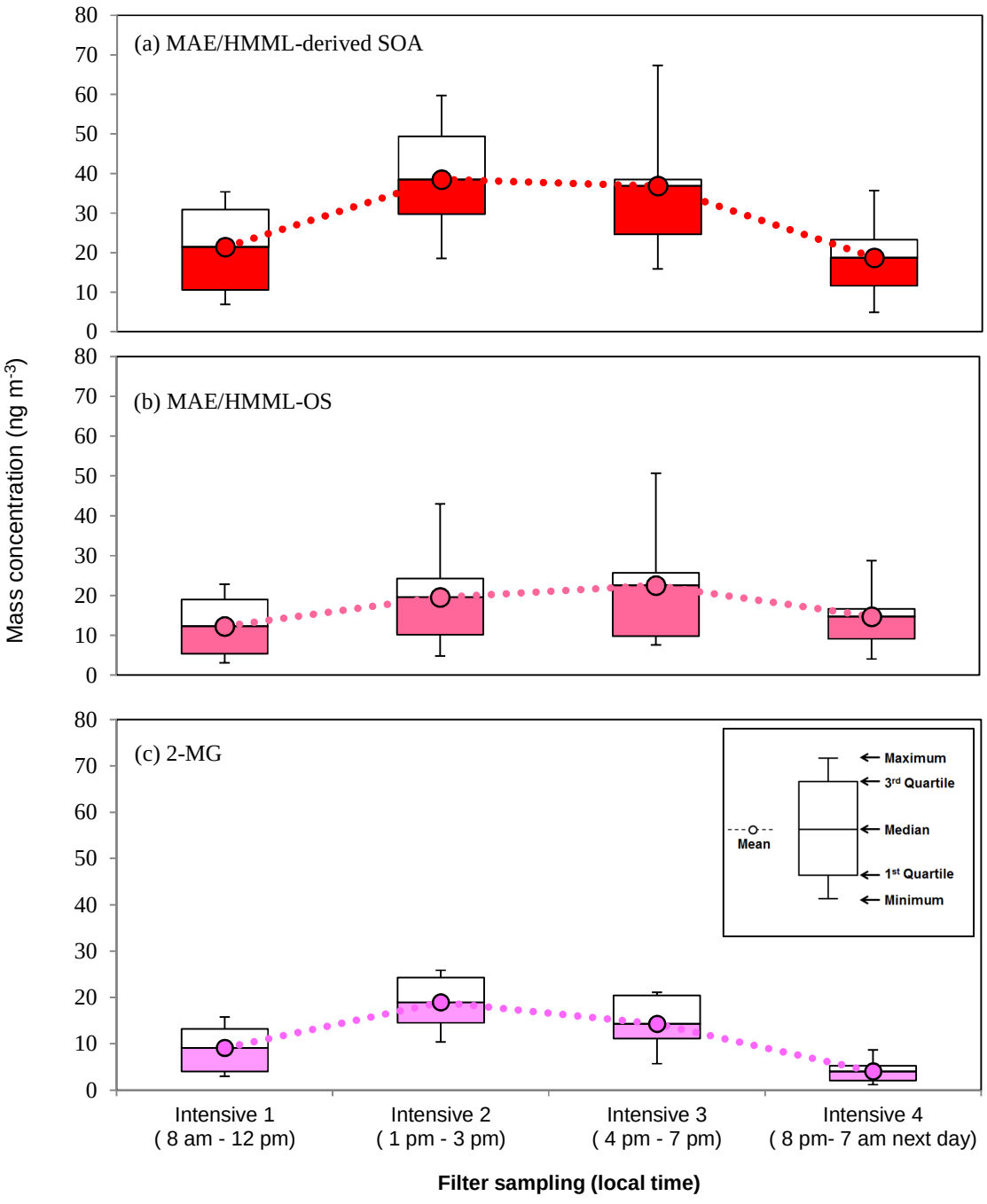

Figure 4. The box-and-whisker plot (n = 15) of (a) MAE/HMML-derived SOA, (b) MAE/HMML-OS, and (c) 2-MG. These demonstrate that the statistical distribution of SOA abundance during each intensive sampling period. No significant variation amongst intensive samples was observed.

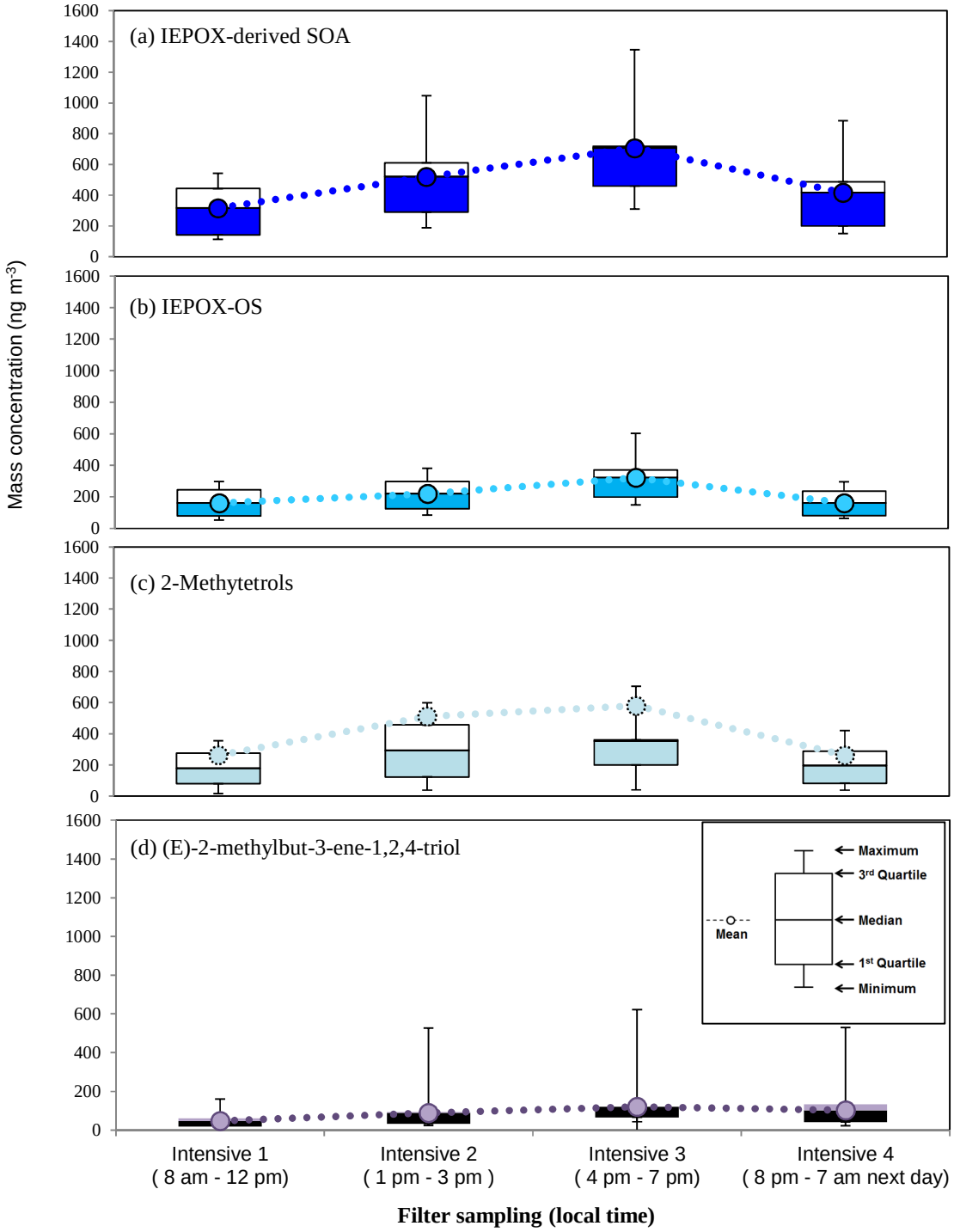

Figure 5. The box-and-whisker plot (n = 15) of (a) IEPOX-derived SOA, (b) IEPOX-OS, (c) 2-methyltetrols, and (d) (E)-2-methylbut-3-ene-1,2,4-triol. These demonstrate that the statistical distribution of SOA abundance during each intensive sampling period. No significant variation amongst intensive samples was observed.

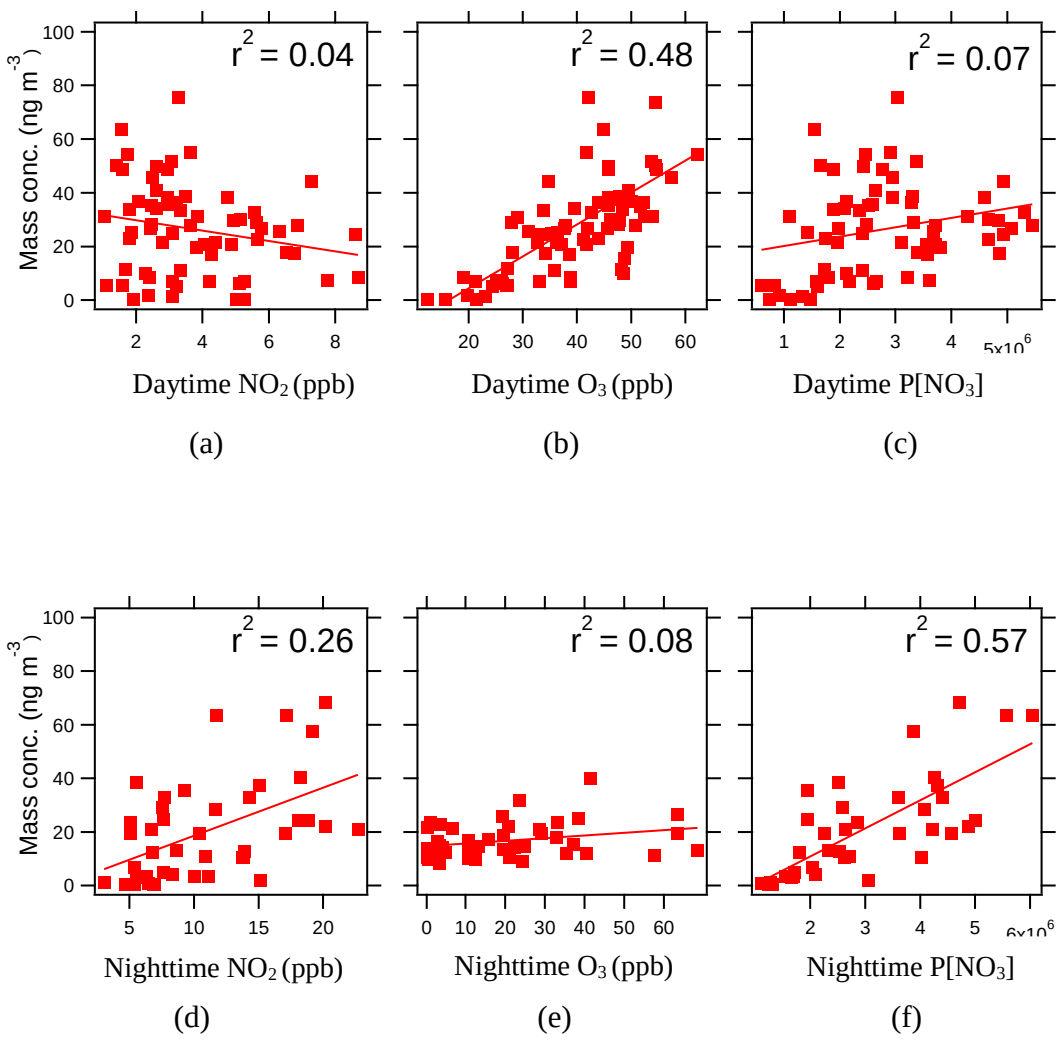

Figure 6. Correlation of MAE/HMML-derived SOA tracers with (a) daytime NO_2, (b) daytime O_3, (c) daytime $P[NO_3]$, (d) nighttime NO_2, (e) nighttime O_3, and (f) nighttime $P[NO_3]$. Nighttime $P[NO_3]$ correlation suggests that NO_3 radical chemistry could explain some fraction of the MAE/HMML-derived SOA tracer concentrations.

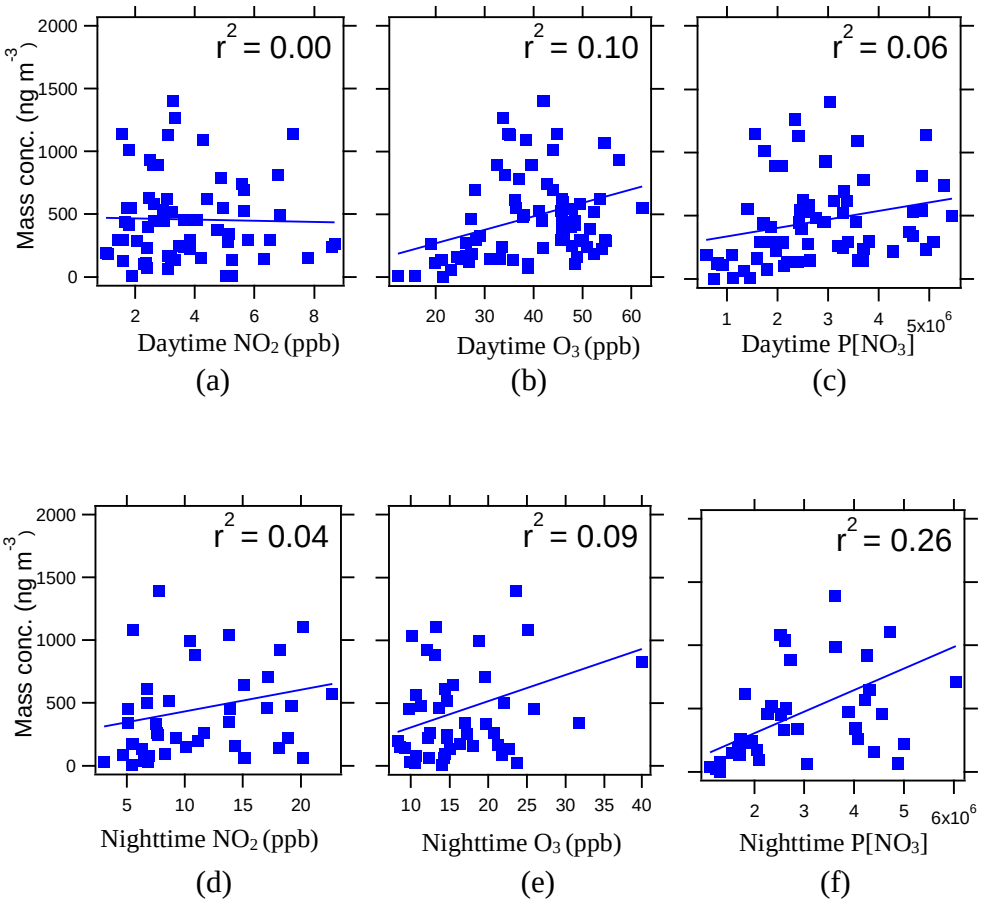

Figure 7. Correlation of IEPOX-derived SOA tracers with (a) daytime NO_2, (b) daytime O_3, (c) daytime $P[NO_3]$, (d) nighttime NO_2, (e) nighttime O_3, and (f) nighttime $P[NO_3]$. Nighttime $P[NO_3]$ correlation suggests that NO_3 radical chemistry could explain some fraction of the IEPOX-derived SOA tracer concentrations. The contribution of nighttime $P[NO_3]$ to IEPOX-derived SOA would be smaller than MAE/HMML-derived SOA due to the weaker correlation.